

# Quantum Field Theory in the Limit $x \ll 1$ <sup>1</sup>

C.R. Stephens<sup>2</sup>, A. Weber<sup>3</sup>, J.C. López Vieyra<sup>4</sup> and P.O. Hess<sup>5</sup>

Instituto de Ciencias Nucleares, UNAM,  
Circuito Exterior C.U., A. Postal 70-543,  
04510 México D.F., Mexico,  
Tel. (52)-5-622 46 90, Fax (52)-5-622 46 93

**Abstract:** The asymptotic high momentum behaviour of quantum field theories with cubic interactions is investigated using renormalization group techniques in the asymmetric limit  $x \ll 1$ . Particular emphasis is paid to theories with interactions involving more than one field where it is found that a matrix renormalization is necessary. Asymptotic scaling forms, in agreement with Regge theory, are derived for the elastic two-particle scattering amplitude and verified in one-loop renormalization group improved perturbation theory, corresponding to the summation of leading logs to all orders. We give explicit forms for the Regge trajectories of different scalar theories in this approximation and determine the signatures.

PACS numbers: 11.10.Gh, 11.10.Jj, 11.10.St, 12.40.Nn

Keywords: renormalization group, Regge limit, high-energy behaviour

---

<sup>1</sup>This work was supported by Conacyt grant 3298P-E9608.

<sup>2</sup>e-mail: stephens@nuclecu.unam.mx

<sup>3</sup>Supported during part of the work by fellowships of the DAAD and the Mexican Government; e-mail: axel@nuclecu.unam.mx

<sup>4</sup>e-mail: vieyra@nuclecu.unam.mx

<sup>5</sup>e-mail: hess@nuclecu.unam.mx

# 1 Introduction

Asymptotic behaviour at large energy scales, or alternatively small distance scales, has been, and will continue to be, one of the prime foci for research in quantum field theory, and therefore by implication in particle physics. One obvious example of where short distance physics plays a crucial role is in the perturbative treatment of continuum quantum field theory wherein the existence of quantum fluctuations leads to the apparent nonsense of ultraviolet divergences. The renormalization programme, in general, has dealt with this problem very successfully in a physically important class of field theories.

One of the most important members of this class of theories is QCD which possesses the important property of being asymptotically free in the ultraviolet. The renormalization group (RG) has proved to be an extremely powerful tool in accessing this limit via its non-perturbative resummation of classes of Feynman diagrams. In particular RG methods, often combined with other non-perturbative techniques such as the operator product expansion, have been very successful in describing the logarithmic corrections seen experimentally in deep inelastic scattering (see ref. [1] for a review). Asymptotically free theories have a very important advantage relative to others — that a description of their true high energy behaviour does not depend on lower energy “infrared scales”. This means that a very simple renormalization procedure such as minimal subtraction is sufficient to access all the relevant physics associated with the fixed point and corrections to it.

In terms of asymptotic behaviour as a function of momentum use of the RG, as based on minimal subtraction for example, has essentially been restricted to symmetric limits where all momenta are scaled equally by some factor. Such a symmetric limit is associated with isotropic scale changes and has been sufficient to describe the deep-inelastic limit. Very often however systems are anisotropic and/or inhomogeneous or are probed in an asymmetric way. This is precisely the case when describing semi-hard processes in QCD in the limit  $Q^2 \gg \Lambda_{QCD}^2$ ,  $x \ll 1$  where  $Q^2$  and  $x$  are the Bjorken scaling variables. This corresponds to the diffractive, or Regge limit, which is of great experimental relevance (see for instance ref. [2] for recent results from HERA), and where standard RG improved perturbation theory breaks down. Various methods have been proposed and used to tackle this problem with varying degrees of success. One of the most common is the summation of leading logs [3] via an inspection of the perturbation expansion, a technique which has a long history (see for instance ref. [4] and references therein). Besides an intrinsic degree of arbitrariness, summing sets of logs can be quite difficult combinatorially. Other methods include: multiperipheral models [5], absorption models [6] and eikonal models [7].

There is also a strong secondary motivation for studying the Regge limit that is associated with the remarkable property of Regge theory that relates high energy behaviour in one channel with infrared behaviour in the crossed channel, and in particular the physics of bound states, the solutions of the equation  $\alpha(s = m^2) = l$  yielding the masses of the  $s$ -channel bound states,  $l$  being the angular momentum of the state.

In this paper we wish to present an RG methodology that is quite general and can describe both symmetric (hard) and asymmetric (semi-hard) asymptotic limits of the high momentum behaviour in quantum field theory (some preliminary results appeared in ref. [8]). In particular we will treat quite generally “cubic” field theories, wherein the asymmetric Regge

limit is a particularly interesting one. We will illustrate the principal concepts in the context of scalar theories to avoid complications due to spin and gauge invariance. We emphasize however that the methodology is equally applicable to these cases too. RG methods have been used in the context of Reggeonic field theory [9], however, the latter is an effective field theory wherein one makes an ansatz for the theory that describes the Reggeonic effective degrees of freedom. For instance, in this approach the “bare” Regge slope and intercept are not calculated but are input data.

One of the reasons the RG does not seem to have been utilized to investigate asymmetric asymptotic behaviour is its association with the problem of ultraviolet divergences. In the Regge limit the breakdown of perturbation theory has nothing to do with the latter. However, terms such as  $\ln s$  or  $\ln t$ , in the limits  $s, t \rightarrow \infty$ , do lead to divergences. These divergences in contradistinction to symmetric short distance behaviour are very asymmetric. The reason they appear can be traced to the nature of the effective degrees of freedom in the problem. For small  $s$  and  $t$  they are four-dimensional, whereas in the Regge limit, as is well known, there is a “kinematic” dimensional reduction to two dimensions owing to the extreme anisotropy between the longitudinal and transverse sectors. This type of dimensional reduction has much in common with “geometric” dimensional reductions, such as occur in finite temperature field theory in the vicinity of a second order phase transition [10]. Such crossovers between effective degrees of freedom of one type and another, qualitatively completely different, are ubiquitous in physics. Indeed the crossover between asymptotic freedom and confinement offers a perfect paradigm. Given the close relationship, via Regge theory, between high energy behaviour in one channel and low energy behaviour in the crossed channel we thus expect the results herein to be of use in understanding the crossover between bound states and unbound states. Yet a third motivation, additional to studying high momentum behaviour and the physics of bound states is that of studying the crossover between string-like behaviour and particle-like behaviour. Study of the Regge limit and the subsequent introduction of the Veneziano model led directly to a string formulation. Now the emphasis is more on deriving point-particle field theories as effective field theories in the low energy limit of string theory rather than vice-versa. It remains a challenge however to understand fully to what extent a point particle field theory may manifest stringy behaviour in some effective field theory limit.

To describe systematically such crossovers using RG methods one requires a RG that can interpolate between different effective degrees of freedom as a function of “scale”, where scale could mean temperature, momentum, size etc. Such an RG, that can be applied to a myriad of other crossover situations, has been developed under the name of “environmentally friendly” renormalization [11] in recognition of the fact that a crossover very often can be thought of as taking place due to the effect of some “environmental” parameter, such as temperature. Using these methods it has been possible, for instance, to access the dimensional crossover in finite temperature field theory [12] between an effective four dimensional theory at low temperatures to an effectively three dimensional theory near a second or weakly first order phase transition. In this paper we will apply the philosophy and techniques of environmentally friendly renormalization to an investigation of the asymmetric, high momentum limit of “cubic” quantum field theories.

The format of the paper will be as follows: in section 2 we will give a brief discussion

of relativistic Regge theory and derive the non-perturbative asymptotic scaling form for the two-particle on-shell scattering amplitude in the large- $t$  limit. In section 3 we will introduce the RG techniques we will use to access the Regge limit, while section 4 deals with the case of interactions involving different fields leading to mixing between the effective vertices in the asymptotic regime. In section 5 we will treat fully to one loop the example of a scalar, non-gauge version of QED with interaction  $\phi^\dagger\phi\psi$ . Finally in section 6 we will discuss the results found and draw some conclusions. There are also three appendices: one showing that our techniques also work to two loops, another proving that indeed to one loop our renormalization sums up all leading logs whilst the third gathers together some technical results needed in the main text.

## 2 Relativistic Regge Theory

In this section we will briefly review the fundamentals of Regge theory for relativistic particle scattering. A more detailed account can be found, for instance, in ref. [13]. One advantage of Regge theory is that it yields totally non-perturbative information, albeit at the expense of several assumptions, about the asymptotic forms of scattering amplitudes. Additionally it will yield directly the connection between bound state information in one channel with high energy behaviour in the crossed channel.

Let  $A(s, t)$  be the amplitude for the scattering of two spinless bosons, where the two outgoing bosons may be different from the incoming ones.  $A(s, t)$  is given by the amputated connected four-point function  $\tilde{\Gamma}^{ijkl}$  with the external momenta on mass shell, and  $s$  and  $t$  are the Mandelstam variables. For the sake of simplicity, in this section we will write down the formulas for the case where the masses  $m$  of all external particles are equal.

The central assumption of Regge theory (and of S-matrix theory in general) is that  $A(s, t)$  is an analytic function of  $s$  and  $t$  and satisfies a dispersion relation of the following form:

$$A(s, t) = \frac{1}{\pi} \int_{t_0}^{\infty} dt' \frac{A_t(s, t')}{t' - t} + \frac{1}{\pi} \int_{u_0}^{\infty} du' \frac{A_u(s, u')}{u' - u}, \quad (1)$$

where  $A_t$  and  $A_u$  are the absorptive parts of  $A$ , i.e. the discontinuities across the cuts in the  $t$  and  $u$  channels, and are assumed to be analytic themselves with the respective cuts. The third Mandelstam variable  $u$  is given in terms of the other two by the on-shell relation

$$s + t + u = 4m^2. \quad (2)$$

The positions of the branch points in (1) are  $t_0 = u_0 = 4m^2$ , provided that there are no lighter particles in the theory, hence the cuts lie outside the physical region  $t, u < 0$  for  $s$ -channel scattering.

The exchange of particles leads to additional pole terms in (1), which are usually omitted in the dispersion relation. They play no role in the following discussion. Similarly, subtractions may be necessary in (1) due to the behaviour of  $A(s, t)$  for asymptotic values of  $t$ , but they will not affect the following reasoning.

For  $s > 4m^2$ , we decompose  $A$  into partial waves,

$$A(s, t) = A(s, z) = \sum_{l=0}^{\infty} (2l + 1) a_l(s) P_l(z), \quad (3)$$

where  $z$  is the cosine of the scattering angle in the center-of-mass system for  $s$ -channel scattering,

$$z = 1 + \frac{2t}{s - 4m^2} = -1 - \frac{2u}{s - 4m^2}. \quad (4)$$

We can rewrite the dispersion relation (1) in terms of the scattering angle as

$$A(s, z) = \frac{1}{\pi} \int_{1+2t_0/(s-4m^2)}^{\infty} dz' \frac{A_t(s, z')}{z' - z} + \frac{1}{\pi} \int_{-1-2u_0/(s-4m^2)}^{-\infty} dz' \frac{A_u(s, -z')}{z' - z}, \quad (5)$$

from where we extract the partial wave amplitudes

$$a_l(s) = \frac{1}{\pi} \int_{1+2t_0/(s-4m^2)}^{\infty} dz' A_t(s, z') Q_l(z') - \frac{1}{\pi} \int_{-1-2u_0/(s-4m^2)}^{-\infty} dz' A_u(s, z') Q_l(-z') \quad (6)$$

with the Legendre functions of the second kind  $Q_l$ .

The partial wave amplitudes  $a_l$  do not allow directly for a Sommerfeld-Watson transform due to the behaviour of  $Q_l(z)$  for large  $|l|$ , and we have to introduce two different amplitudes  $a^{\pm}(l, s)$  with “signatures”  $+$  and  $-$ , respectively. They are given by the Froissart-Gribov formula [14]

$$a^{\pm}(l, s) = \frac{1}{\pi} \int_{1+2t_0/(s-4m^2)}^{\infty} dz' A_t(s, z') Q_l(z') \pm \frac{1}{\pi} \int_{-1-2u_0/(s-4m^2)}^{-\infty} dz' A_u(s, z') Q_l(z'). \quad (7)$$

Both amplitudes can be continued uniquely to complex values of  $l$  by virtue of Carlson’s theorem (see, e.g., ref. [15]). As we will see later,  $a^+$  is associated with physical states of even angular momentum and  $a^-$  with odd angular momentum ones.

The corresponding scattering amplitudes

$$A^{\pm}(s, z) = \sum_{l=0}^{\infty} (2l+1) a^{\pm}(l, s) P_l(z) \quad (8)$$

then allow separately for a Sommerfeld-Watson transform [16]. Assuming that the partial wave amplitudes  $a^{\pm}$ , considered as analytic functions in the complex  $l$ -plane, possess simple poles at

$$l = \alpha_i^{\pm}(s), \quad \text{Re}(\alpha_i^{\pm}(s)) > -\frac{1}{2}, \quad (9)$$

we get the result

$$\begin{aligned} A^{\pm}(s, z) &= \frac{i}{2} \int_{-1/2-i\infty}^{-1/2+i\infty} dl \frac{(2l+1) a^{\pm}(s, l) P_l(-z)}{\sin(\pi l)} \\ &\quad - \pi \sum_i \frac{(2\alpha_i^{\pm}(s) + 1) \beta_i^{\pm}(s) P_{\alpha_i^{\pm}(s)}(-z)}{\sin(\pi \alpha_i^{\pm}(s))}, \end{aligned} \quad (10)$$

where  $\beta_i^{\pm}(s)$  is the residue of  $a^{\pm}$  at  $l = \alpha_i^{\pm}(s)$ .

In the case that subtractions are necessary in (1), we have to assume in addition the absence of “elementary poles” for (10) to be valid. Furthermore, since in fact the functions  $a^\pm$  possess besides simple poles also branch cuts in the  $l$ -plane giving rise to additional contributions in (10), we will assume that in the asymptotic limit to be discussed in the following, the dominant contributions originate from the poles only. The poles  $\alpha_i^\pm(s)$  of  $a^\pm$  are known as Regge poles [17], while the functional dependence of a Regge pole on  $s$  is referred to as its Regge trajectory.

Let us now consider the limit  $z \rightarrow \infty$ , which for  $s > 4m^2$  corresponds to  $t \rightarrow \infty$ . Using the asymptotic behaviour of the Legendre functions (for this and other properties of the Legendre functions see, for instance, ref. [18]),

$$P_\alpha(z) \approx \frac{\Gamma(2\alpha + 1)}{2^\alpha (\Gamma(\alpha + 1))^2} z^\alpha, \quad |z| \rightarrow \infty, \quad (11)$$

we have from (10) that asymptotically

$$A^\pm(s, z) = \sum_i \frac{\beta_i'^\pm(s)}{\sin(\pi\alpha_i^\pm(s))} z^{\alpha_i^\pm(s)}, \quad (12)$$

where

$$\beta_i'^\pm(s) = -\frac{\pi\Gamma(2\alpha_i^\pm(s) + 2)\beta_i^\pm(s)e^{-i\pi\alpha_i^\pm(s)}}{2^{\alpha_i^\pm(s)}(\Gamma(\alpha_i^\pm(s) + 1))^2}. \quad (13)$$

We can then determine the asymptotic behaviour of the full scattering amplitude,

$$A(s, z) = \frac{1}{2} (A^+(s, z) + A^+(s, -z) + A^-(s, z) - A^-(s, -z)). \quad (14)$$

Plugging in (12), we obtain

$$A(s, z) = \sum_i \frac{\beta_i'^+(s)(1 + e^{i\pi\alpha_i^+(s)})}{2\sin(\pi\alpha_i^+(s))} z^{\alpha_i^+(s)} + \sum_i \frac{\beta_i'^-(s)(1 - e^{i\pi\alpha_i^-(s)})}{2\sin(\pi\alpha_i^-(s))} z^{\alpha_i^-(s)} \quad (15)$$

for  $z \rightarrow \infty$ . Replacing  $z$  via (4), we have asymptotically

$$A(s, t) = \sum_i \frac{\tilde{\beta}_i'^+(s)(1 + e^{i\pi\alpha_i^+(s)})}{2\sin(\pi\alpha_i^+(s))} t^{\alpha_i^+(s)} + \sum_i \frac{\tilde{\beta}_i'^-(s)(1 - e^{i\pi\alpha_i^-(s)})}{2\sin(\pi\alpha_i^-(s))} t^{\alpha_i^-(s)} \quad (16)$$

as  $t \rightarrow \infty$ , where

$$\tilde{\beta}_i'^\pm(s) = \left( \frac{2}{s - 4m^2} \right)^{\alpha_i^\pm(s)} \beta_i'^\pm(s). \quad (17)$$

Up to now, we have shown the validity of (16) for  $s > 4m^2$  only. Due to the analyticity of  $A_t$  and  $A_u$ , however, we can analytically continue in  $s$  to the region  $s < 4m^2$ , starting with (7) in the form

$$\begin{aligned} a^\pm(l, s) &= \frac{1}{\pi} \int_{t_0}^{\infty} \frac{2 dt'}{s - 4m^2} A_t(s, t') Q_l \left( 1 + \frac{2t'}{s - 4m^2} \right) \\ &\pm \frac{1}{\pi} \int_{u_0}^{\infty} \frac{2 du'}{s - 4m^2} A_u(s, u') Q_l \left( 1 + \frac{2u'}{s - 4m^2} \right). \end{aligned} \quad (18)$$

Then (16) remains unchanged in the limit  $t \rightarrow \infty$ , with

$$\tilde{\beta}_i^\pm(s) = -\frac{\pi\Gamma(2\alpha_i^\pm(s) + 2)\beta_i^\pm(s)e^{-2i\pi\alpha_i^\pm(s)}}{(\Gamma(\alpha_i^\pm(s) + 1))^2(4m^2 - s)\alpha_i^\pm(s)} \quad (19)$$

for  $s < 4m^2$ . Note that the phase factors in (13–19) follow from taking  $s$  on the upper edge of the right-hand cut in the  $s$ -plane, i.e.  $s \rightarrow s + i\epsilon$  for  $s > 4m^2$ , and likewise for  $t$ .

For comparison with our results to be described in sections 3, 4 and 5 we determine the  $t$ - and  $u$ -contributions in (16). The latter are identified with the contributions to  $A(s, t)$  from the corresponding cuts in (1), and can be associated with certain classes of diagrams in the limit  $t \rightarrow \infty$ . Following the derivation of (16), we can easily identify the terms

$$\sum_i \frac{\tilde{\beta}_i^+(s)}{2 \sin(\pi\alpha_i^+(s))} t^{\alpha_i^+(s)} + \sum_i \frac{\tilde{\beta}_i^-(s)}{2 \sin(\pi\alpha_i^-(s))} t^{\alpha_i^-(s)} \quad (20)$$

with the  $t$ -contributions, while

$$\sum_i \frac{\tilde{\beta}_i^+(s)e^{i\pi\alpha_i^+(s)}}{2 \sin(\pi\alpha_i^+(s))} t^{\alpha_i^+(s)} - \sum_i \frac{\tilde{\beta}_i^-(s)e^{i\pi\alpha_i^-(s)}}{2 \sin(\pi\alpha_i^-(s))} t^{\alpha_i^-(s)} \quad (21)$$

arise from the  $u$ -contributions.

Formula (16) is the main result of Regge theory. It states that the asymptotic behaviour is determined by the Regge trajectories, and that the dominant contribution comes from the right-most Regge pole  $\alpha_0^\pm(s)$  in the complex  $l$ -plane. The Regge limit  $t \rightarrow \infty$  corresponds for  $s < 0$  to the physical high-energy limit for scattering in the  $t$ -channel. For  $s > 0$ , the scattering amplitude is not experimentally accessible, but has to be obtained by analytic continuation from the physical region.

From (16) we see that  $A$  has a pole in  $s$  whenever  $\alpha_i^+(s)$  ( $\alpha_i^-(s)$ ) equals an even (odd) non-negative real integer. The signature factor

$$1 \pm e^{i\pi\alpha_i^\pm(s)} \quad (22)$$

leads to the cancellation of the poles for odd  $\alpha_i^+(s)$  and even  $\alpha_i^-(s)$ . We can read off from (10) that the existence and position of these poles is independent of the value of  $z$  (or  $t$ ). In particular, they occur inside the region  $-1 < z < 1$  and therefore correspond to bound states (for  $s < 4m^2$ ) or resonances ( $\text{Re}(s) > 4m^2$ ) in the  $s$ -channel with the respective angular momenta. In this way, Regge theory provides a link between the high-energy behaviour in one channel and bound state formation in the crossed channel.

We will conclude this section with a qualitative description of the Regge trajectories in the complex  $l$ -plane. The leading trajectory  $\alpha_0^\pm(s)$  starts out at  $l = -1$  for  $s \rightarrow -\infty$ , and with increasing  $s$  moves along the real axis towards larger values of  $l$ . If we assume the absence of vacuum condensation, it should cross  $l = 0$  (the first physical state) with a positive value of  $s$ . It then produces a series of excited bound states with increasing angular momenta, until at  $s = 4m^2$  we find a branch point in  $s$ , and the trajectory moves into the upper half plane. It may stay close to the real axis for a while, producing resonances with

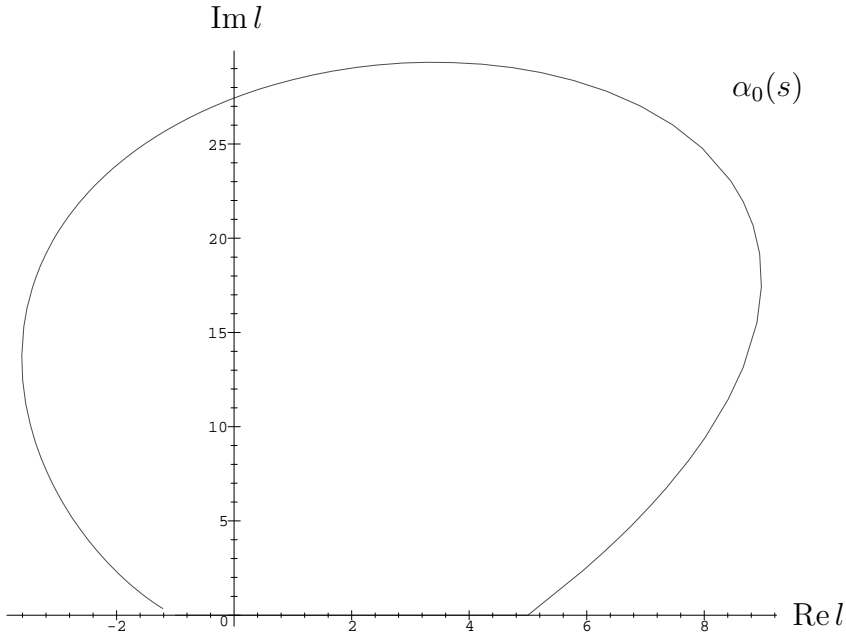


Figure 1: A representative leading Regge trajectory  $\alpha_0$  in the complex  $l$ -plane, starting and ending at  $l = -1$ .

angular momenta corresponding to the real parts of  $l$ , whenever the real part passes through an integer value. Finally, the Regge trajectory will return through the upper half plane to  $l = -1$  for  $s \rightarrow \infty$ . Fig. 1 shows a “typical” trajectory in the complex  $l$ -plane, corresponding to an interaction through exchange of massive particles.

How far the trajectory penetrates the right half plane depends on the dynamics of the theory. It may produce just one bound state at  $l = 0$ , or only one resonance, or no physical state at all. There are also Regge trajectories in the case of repulsive interactions. In this case the leading trajectory, starting at  $l = -1$ , would move to the left in the complex plane, eventually returning to  $l = -1$  through the lower half plane. It will never produce bound states nor resonances. Finally, there are in general subleading Regge trajectories which behave similarly to the leading trajectory, but start out at lower values  $l = -2, -3, -4, \dots$  for  $s \rightarrow -\infty$ .

### 3 Scaling and the Renormalization Group

In this section we will present the basic ideas behind the renormalization we will use. In particular we will introduce the concepts of environmentally friendly renormalization within the simplified context of a cubic scalar field theory with Lagrangian

$$\mathcal{L} = \frac{1}{2} \partial_\mu \phi \partial_\mu \phi + \frac{1}{2} m_B^2 \phi^2 + \frac{g_B}{6} \phi^3 . \quad (23)$$

The index  $B$  will be used to denote bare quantities throughout.



We will illustrate the formalism within the context of “cubic” scalar theories for reasons of sheer simplicity, and because cubic couplings also appear in gauge theories. Although these bosonic theories suffer from vacuum instability, perturbation theory around the “perturbative” vacuum is well-defined order by order. Furthermore, they have been used extensively as model theories to investigate Regge behaviour in perturbation theory (see, for instance, ref. [4]). In principle, one may always think of adding a stabilizing  $\phi^4$  term but with an arbitrarily small coupling such that it plays no role in what we are about to discuss.

The general notation we will use will be the following: an  $n$ -point connected (bare) Greens function will be denoted,  $G_B^{i_1\dots i_n}(p_1, \dots, p_n)$  where we use the superscript notation  $i_1\dots i_n$  to denote the external legs, i.e.  $i_1, \dots, i_n$  can take different values depending on the field content of the theory. For instance, in  $\phi^3$  theory,  $i_k = \phi$  for all  $k$ . For a theory with interaction term  $\phi^\dagger\phi\psi$ ,  $i_k$  can represent  $\phi$ ,  $\phi^\dagger$  or  $\psi$ . Thus  $G_B^{\phi\phi}$  represents propagation of the charged  $\phi$ -particle and  $G_B^{\phi^\dagger\phi^\dagger}$  propagation of the corresponding antiparticle, whilst  $G_B^{\psi\psi}$  represents propagation of the neutral particle  $\psi$ .

Rather than deal with the connected Greens functions we will find it useful to consider the quantities  $\tilde{\Gamma}_B^{i_1\dots i_n}(p_1, \dots, p_n)$  which are closely related to the  $S$ -matrix elements and are obtained from the connected Greens functions by removing the external legs,

$$\tilde{\Gamma}_B^{i_1\dots i_n}(p_1, \dots, p_n) = \prod_{k=1}^n \Gamma_B^{i_k i_k}(p_k) G_B^{i_1\dots i_n}(p_1, \dots, p_n). \quad (24)$$

The relation to fully one-particle irreducible Greens functions is found using the standard “tree theorem”. For instance, for the four-point function introduced in the last section one has the decomposition

$$\begin{aligned} \tilde{\Gamma}_B^{ijkl}(s, t, u) &= \Gamma_B^{ijkl}(s, t, u) + \Gamma_B^{ijm}(s) G_B^{mm}(s) \Gamma_B^{mkl}(s) \\ &\quad + \Gamma_B^{ikm}(t) G_B^{mm}(t) \Gamma_B^{mjl}(t) + \Gamma_B^{ilm}(u) G_B^{mm}(u) \Gamma_B^{mjk}(u), \end{aligned} \quad (25)$$

or diagrammatically

$$\tilde{\Gamma}_B^{ijkl} = \begin{array}{c} i \\ \diagdown \\ \bigcirc \\ \diagup \\ j \\ k \quad l \end{array} = \begin{array}{c} \diagdown \\ \bigcirc \\ \diagup \end{array} + \begin{array}{c} \diagdown \\ \bigcirc \\ \diagup \\ \bigcirc \\ \diagdown \\ \diagup \end{array} + \begin{array}{c} \diagdown \\ \bigcirc \\ \diagup \\ \bigcirc \\ \diagdown \\ \diagup \end{array} + \begin{array}{c} \diagdown \\ \bigcirc \\ \diagup \\ \bigcirc \\ \diagdown \\ \diagup \end{array} + \begin{array}{c} \diagdown \\ \bigcirc \\ \diagup \\ \bigcirc \\ \diagdown \\ \diagup \end{array} \quad (26)$$

As indicated above, on mass shell  $\tilde{\Gamma}_B^{ijkl}$  depends on the momenta only through the Mandelstam variables  $s, t, u$ , which are related by (2).

We will first consider the large- $t$  limit of the four-point function, and afterwards the “dual” limit  $s \rightarrow \infty$ . It is then convenient to consider the particles  $k$  and  $l$  as incoming and  $i$  and  $j$  as outgoing, i.e. the  $s$ -channel process is  $kl \rightarrow ij$ . Consequently we define

$$s = -(p_1 + p_2)^2, \quad t = -(p_1 - p_3)^2, \quad u = -(p_1 - p_4)^2, \quad (27)$$

working in Euclidean space throughout.<sup>6</sup> The minus signs in (27) are introduced for convenience, in order that the Mandelstam variables take their usual Minkowskian values.

<sup>6</sup>Note that the present definitions of the Mandelstam variables differ by a sign from the ones used in ref. [8].

Let us first discuss the philosophy behind the renormalization. To illustrate this we will consider the lowest order functions,  $\tilde{\Gamma}_B^{\phi\phi}$ ,  $\tilde{\Gamma}_B^{\phi\phi\phi}$  and  $\tilde{\Gamma}_B^{\phi\phi\phi\phi}$  for  $\phi^3$ . Explicitly, to one loop

$$\tilde{\Gamma}_B^{\phi\phi}(p_1, p_2, m_B, g_B, \Lambda) = \text{---} + \text{---} \bigcirc \text{---} \quad (28)$$

$$\tilde{\Gamma}_B^{\phi\phi\phi}(p_1, p_2, p_3, m_B, g_B, \Lambda) = \text{---} \text{---} \text{---} + \text{---} \triangle \text{---} \quad (29)$$

$$\begin{aligned} \tilde{\Gamma}_B^{\phi\phi\phi\phi}(p_1, p_2, p_3, p_4, m_B, g_B, \Lambda) = & \text{---} \text{---} \text{---} \text{---} + \text{---} \bigcirc \text{---} \text{---} \text{---} + (s \text{ and } u \text{ perms}) + \\ & \text{---} \bigcirc \text{---} \text{---} \text{---} + \text{---} \bigcirc \text{---} \text{---} \text{---} + (s \text{ and } u \text{ perms}) + \\ & \text{---} \square \text{---} + \text{---} \text{---} \text{---} \text{---} + \text{---} \text{---} \text{---} \text{---} \end{aligned} \quad (30)$$

where the  $s$  and  $u$  permutations indicate the same diagrams but in the crossed channels. We have introduced an ultraviolet cutoff in order to regularize any UV divergences present. If we restrict attention to four dimensions for simplicity then the only UV divergence occurs in  $\text{---} \bigcirc \text{---}$  which diverges logarithmically. This UV divergence can be removed in the standard fashion via a normalization condition, for instance that the renormalized two-point vertex function have a zero on the mass shell, i.e.

$$\tilde{\Gamma}_B^{\phi\phi}(p^2 = -m^2, m, g) = 0. \quad (31)$$

After this mass renormalization, then as far as UV divergences are concerned the theory is totally finite. However, we will now consider the large momentum behaviour of the theory. In particular we will consider two-particle scattering in the asymmetric limit  $t \rightarrow \infty$  for fixed  $s$ .

In this limit and considering the on-shell amplitude we can classify the one-loop diagrams according to whether they contain a factor of  $\ln t$ , a factor of  $\ln(-t)$ , or are “finite”. This separation can in principle be carried out to all orders leading to the following decomposition for  $\Gamma_B^{ijkl}$ :

$$\Gamma_B^{ijkl}(s, t, u) = A_{B,t}^{ijkl}(s, t) + A_{B,u}^{ijkl}(s, u) + A_{B,s}^{ijkl}(t, u), \quad (32)$$

where  $A_{B,t}^{ijkl}$  includes the one-particle irreducible diagrams with powers of  $\ln(-t)$  (“ $t$ -contributions”),  $A_{B,u}^{ijkl}$  includes the diagrams with powers of  $\ln t$  (“ $u$ -contributions”), and  $A_{B,s}^{ijkl}$  includes the remaining diagrams (“ $s$ -contributions”). There is of course an analogous decomposition associated with the limits  $s \rightarrow \infty$  and  $u \rightarrow \infty$ .

For the  $\phi^3$  theory at one loop  $A_{B,t}^{ijkl}$  is given by the planar box diagram in (30),  $A_{B,u}^{ijkl}$  by the first and  $A_{B,s}^{ijkl}$  by the second “crossed” box. The relation of the present definition of  $t$ - and  $u$ -contributions to the one given in the last section (above formula (20)) is easy to see: The planar box diagram has a threshold cut in  $t$ , and the first crossed box diagram a corresponding cut in  $u$ . Consequently they determine to one loop the contributions from

the cuts in (1). The second crossed box diagram possesses threshold cuts in  $t$  and  $u$ , but its contributions are suppressed in the limit  $t \rightarrow \infty$ .

It is worth mentioning here one subtlety associated with the above: at some order in the loop expansion there will appear terms with logarithms that are associated with singularities in the complex angular momentum plane other than Regge poles. For instance, in the present theory at five loops the non-planar ladder type diagram with three iterated crosses will yield a term of the form  $\sim g_B^{12} t^{-1} \ln t$  which arises from a pinch type singularity rather than an end-point singularity in the integration over Feynman parameters and should be interpreted as a contribution to an essential singularity related to the Gribov-Pomeranchuk phenomenon [4]. There will also be terms that correspond to Regge cuts, once again these will be associated with non-planar diagrams. One can take different attitudes towards this problem. One is simply to include them as contributions to the functions  $A_{B,t}^{ijkl}$  even though they really correspond to singularities other than Regge poles. This is in some sense analogous to the ‘‘poles only’’ assumption in Regge theory. A more satisfactory resolution is to find appropriate renormalizations that resum the diagrammatic series so as to reproduce the correct type of singularity. Neither way of doing things is ‘‘wrong’’. The RG viewed as a method of reorganization and resummation of perturbative diagrammatic series via reparametrizations cannot give incorrect answers, however, it can give bad approximations. One is seeking a reorganization and resummation that best captures the physics of interest. In the case at hand as these matters are all associated with much higher loop orders we will not consider them further here.

At the level of the functions  $\tilde{\Gamma}_B^{ijkl}$  the natural combinations for investigating the large- $t$  behaviour are the functions  $B_{B,t}^{ijkl}$  for the  $t$ -contributions, and  $B_{B,u}^{ijkl}$  for the  $u$ -contributions, defined as

$$\begin{aligned}
 B_{B,t}^{ijkl}(s, t) &= A_{B,t}^{ijkl}(s, t) + \Gamma_B^{ikm}(t) G_B^{mn}(t) \Gamma_B^{mjl}(t) \\
 &= \text{Diagram 1} + \text{Diagram 2}
 \end{aligned} \tag{33}$$

$$\begin{aligned}
 B_{B,u}^{ijkl}(s, u) &= A_{B,u}^{ijkl}(s, u) + \Gamma_B^{ilm}(u) G_B^{mn}(u) \Gamma_B^{mjk}(u) \\
 &= \text{Diagram 3} + \text{Diagram 4}
 \end{aligned} \tag{34}$$

with an analogous definition for  $B_{B,s}^{ijkl}$  for the  $s$ -contributions. We hence have the decomposition

$$\tilde{\Gamma}_B^{ijkl}(s, t, u) = B_{B,t}^{ijkl}(s, t) + B_{B,u}^{ijkl}(s, u) + B_{B,s}^{ijkl}(t, u). \tag{35}$$

The function  $B_{B,s}^{ijkl}$  contains no large logarithms and will not play an important role in the asymptotic  $t$  behaviour. However, in the large- $t$  limit both  $B_{B,t}^{ijkl}$  and  $B_{B,u}^{ijkl}$  become perturbatively uncontrollable due to large logarithmic corrections. One way to ameliorate this

problem is to try to sum up the large logarithmic terms thus generating a non-perturbative result. This has had a great deal of success but it is heuristically based.

We will here implement an RG approach: Consider the function  $B_{B,t}^{ijkl}(s, t)$  in the large- $t$  limit. In the case of  $\phi^3$  theory, we have explicitly to one loop (omitting the trivial upper indices on  $B_{B,t}$ )

$$B_{B,t}(s, t) = \frac{g_B^2}{-t} + \frac{g_B^4}{-t} K(s) \ln(-t) + O\left(\frac{g_B^4}{t}\right), \quad (36)$$

where the first term on the r.h.s. stems from the  $t$ -channel tree diagram and the second from the planar box diagram, while the contributions of the other one-particle reducible diagrams are relatively suppressed in the large- $t$  limit. The function

$$K(s) = \frac{1}{16\pi^2} \int_0^1 \frac{d\beta}{m^2 - \beta(1-\beta)s} \quad (37)$$

corresponds to a two-dimensional loop integration owing to the well known dimensional reduction associated with the Regge limit (see section 5 for a short derivation of this result). It is clear that in the  $t \rightarrow \infty$  limit the above perturbative expansion is ill defined. Two-loop diagrams lead to terms  $\sim g_B^6 t^{-1} K^2(s) (\ln t)^2$  and  $\sim g_B^6 t^{-1} K'(s) \ln t$  where  $K'$  is  $t$ -independent. Similarly, the function  $B_{B,u}(s, u)$  exhibits the behaviour

$$B_{B,u}(s, u(t, s)) = \frac{g_B^2}{t} + \frac{g_B^4}{t} K(s) \ln t + O\left(\frac{g_B^4}{t}\right). \quad (38)$$

It is clear that in both cases some form of resummation is needed. We will achieve that here by utilizing the RG. It is not difficult to see, due to the fact that there are two sets of large logarithms, one associated with  $B_{B,t}$  and another set with  $B_{B,u}$ , that an overall multiplicative renormalization of the connected four-point function will not be sufficient to make the perturbation series well defined. This is an important point well worth emphasizing here. Normally we associate renormalization with a renormalization of a ‘‘coupling constant’’, i.e. a parameter in the original Lagrangian, or an overall renormalization of a Greens function or vertex function. One may think of this as being associated with the fact that in a certain asymptotic limit there is only one singularity to exponentiate. For instance, in critical phenomena in the massless theory terms of the form  $\epsilon^n (\ln k)^n$  exponentiate to give  $k^{-\eta}$ . In the present case however there is more than one singularity as we shall see. Hence, to exponentiate these singularities one needs to get inside the Greens functions and identify the parts that will renormalize ‘‘naturally’’. In one sense our renormalizations can be seen as just reorganizations of perturbative series. No reorganization is wrong, in that it cannot affect the exact answer, however, to a given order in perturbation theory one type of reorganization may capture much more of the actual behaviour of the entire function than another one.

To achieve an adequate renormalization we will define multiplicative renormalizations of  $B_{B,t}$  and  $B_{B,u}$  separately. Explicitly for  $B_{B,t}$

$$B_t(s, t, g(\kappa), m(\kappa), \kappa) = Z_t B_{B,t}(s, t, g_B, m_B, \Lambda), \quad (39)$$

where the precise form of  $Z_t$  of course depends on the specific normalization condition chosen. Hence,  $B_t$  satisfies an RG equation that follows naturally from the  $\kappa$ -independence of the bare theory,

$$\kappa \frac{d}{d\kappa} B_t(s, t, g(\kappa), m(\kappa), \kappa) = \gamma_t B_t(s, t, g(\kappa), m(\kappa), \kappa), \quad (40)$$

where  $\gamma_t = d \ln Z_t / d \ln \kappa$  is the anomalous dimension of  $B_t$ .

There is of course the question of what are we going to use as our RG scale? The natural answer to this follows from consideration of the physics of the problem. In the large- $t$  regime there is a natural decoupling between the transverse and longitudinal sectors whose consequence is an effective dimensional reduction. In other words the effective degrees of freedom of the system are four dimensional for small  $t$  and two dimensional for large  $t$ . As the physics changes as a function of  $t$ , it is natural to choose an arbitrary, fiducial value of  $t$  as the RG parameter. This is also consistent with the philosophy of environmentally friendly renormalization, i.e. that one should use a renormalization that depends on the “environmental” variable (in this case asymmetric momentum) that induces the crossover. We have assumed in the above renormalizations of the coupling constant and mass. This may or may not be necessary. In the current scalar theory in four dimensions it is not essential as there are no large  $t$ -logarithms in the vertex or mass that require exponentiation. For instance, the one-loop vertex correction is  $\sim g_B^3 (\ln t)^2 / t$ , whilst the one-loop mass correction, after removing the ultraviolet divergence by minimal subtraction, is  $\sim g_B^2 \ln t$ . The former tells us that asymptotically  $g_B$  is a very good approximation to the vertex function. The latter when inserted into the four-point function gives a term of  $O(t^{-2})$  which is negligible compared to  $O(t^{-1})$  terms. In six dimensions however, where the theory is renormalizable, a renormalization of the coupling is essential. In this respect it is more akin to the case of QCD.

With the above choice of the RG scale we have  $\gamma_t = \gamma_t(s, g(\kappa), m(\kappa), \kappa)$  which we will abbreviate in the following as  $\gamma_t(s, \kappa)$ . Integrating equation (40) yields

$$B_t(s, t, g(\kappa), m(\kappa), \kappa) = e^{-\int_{\kappa}^{\rho\kappa} \gamma_t(s, x) \frac{dx}{x}} B_t(s, t, g(\rho\kappa), m(\rho\kappa), \rho\kappa) \quad (41)$$

with an analogous equation for  $B_u$ . As the renormalization scale  $\rho$  is arbitrary we choose  $\rho\kappa = t$ , hence

$$B_t(s, t, g(\kappa), m(\kappa), \kappa) = e^{-\int_{\kappa}^t \gamma_t(s, x) \frac{dx}{x}} B_t(s, t, g(t), m(t), t). \quad (42)$$

Now, in the limit of large  $t$  and  $\kappa$ , as we will see, there exists a “fixed point” wherein  $g(t) \rightarrow g(\infty)$  and  $\gamma_t$  is purely a function of  $s$ , i.e. the total dependence of  $\gamma_t$  on  $\kappa$  through  $g(\kappa)$ ,  $m(\kappa)$  and  $\kappa$  disappears. In that the anomalous dimension,  $\gamma_t$ , depends continuously on  $s$  it might be better to speak of a “line” of fixed points as in the well known case of the two-dimensional XY-model. The fact that the anomalous scaling dimension of  $B_t$  for  $\kappa \rightarrow \infty$  is independent of  $\kappa$  is a direct result of the term by term factorization in perturbation theory in this limit. Note that  $\gamma_t$  will depend on  $g(\infty)$ , which is a non-universal parameter. In this sense the fixed point has more in common with the “infinite mass”, or mean field fixed point in critical phenomena. The fact that fluctuation corrections to  $g(t)$  and  $m(t)$  also vanish in

the large- $t$  limit lends further support to this analogy. For  $\kappa$  and  $t$  sufficiently large we have that

$$B_t(s, t, g(\kappa), m(\kappa), \kappa) = \frac{g^2(t)}{-\kappa} \left(\frac{t}{\kappa}\right)^{\alpha(s)} F_t\left(\frac{s}{t}, \frac{g(t)}{t^{1/2}}, \frac{m(t)}{t^{1/2}}\right), \quad (43)$$

where  $\alpha(s) = -1 - \gamma_t(s)$  and  $F_t$  is a three-variable scaling function. Note that we have removed a factor  $g^2(t)/t$  from  $B_t$ . As a consequence of the irrelevance of the operators associated with  $g(t)$  and  $m(t)$  with respect to the  $t \rightarrow \infty$  “fixed point”, the  $t$ -dependence of the scaling function  $F_t$  disappears to leave an amplitude  $G_t((s/g(\infty), s/m(\infty)))$ , i.e. in terms of momentum variables the amplitude is only a function of  $s$ .<sup>7</sup> Just as the “critical” exponent,  $\alpha$ , depends on a continuous parameter,  $s$ , so too does the “critical amplitude”  $G_t$ . Thus using the RG we can recover the generic form expected via Regge theory, cf. (20).

To obtain the correct ratio of  $t$ - and  $u$ -contributions, we have to consider the role played by the  $Z$  factors. Let us first recall that it is the bare function  $B_{B,t}$  that forms part of the scattering amplitude. According to the above, it is given by

$$B_{B,t}(s, t, g_B, m_B, \Lambda) = \frac{g^2(t)}{-\kappa} \frac{G_t(s)}{Z_t(s, g(\kappa), m(\kappa), \kappa)} \left(\frac{t}{\kappa}\right)^{\alpha(s)}, \quad (44)$$

where we have reexpressed  $Z_t$  in terms of the renormalized parameters. The factor  $Z_t^{-1}$  is obviously necessary to cancel the unphysical  $\kappa$ -dependence. Mathematically,  $Z_t$  is represented by a formal power series. To be able to extract the signature given by the ratio of  $u$ - and  $t$ -contributions, we have to make sure that  $Z_u = Z_t$ , at least in a formal sense. As we will see below and in the following section in more detail, this implies considering the large- $u$  limit for the  $u$ -contributions. Proceeding in exactly the same way as for the  $t$ -contributions above (just replacing  $t$  by  $u$  everywhere) we find for the function  $B_u$

$$B_u(s, u, g(\kappa), m(\kappa), \kappa) = e^{-\int_{\kappa}^u \gamma_u(s, x) \frac{dx}{x}} B_u(s, u, g(u), m(u), u). \quad (45)$$

Once again in the limit of large  $u$  and  $\kappa$  for fixed  $s$ ,  $\gamma_u$  is independent of  $\kappa$  and the corresponding scaling function  $F_u \rightarrow G_u(s)$ . To one loop in the large- $t$  limit, as we will see,  $\gamma_t = \gamma_u$  and  $G_t = G_u$ . It is apparent that this holds to all orders in the case of the simple theory under consideration, since for every diagram that contributes to  $\gamma_t$  and  $G_t$  there is a crossed diagram with the incoming or outgoing legs interchanged that contributes identically in the large- $u$  limit to  $\gamma_u$  and  $G_u$ .

We can now replace  $u$  by  $-t$ , to be interpreted as  $e^{i\pi}t$  (see below), and add the  $t$ - and  $u$ -contributions to find (with  $Z \equiv Z_t = Z_u$  and similarly for  $G$ )

$$\tilde{\Gamma}_B^{\phi\phi\phi\phi}(s, t) = \frac{g^2(t)}{-\kappa} \frac{G(s)(1 + e^{i\pi\alpha(s)})}{Z(s, g(\kappa), m(\kappa), \kappa)} \left(\frac{t}{\kappa}\right)^{\alpha(s)} + B_s(t, u), \quad (46)$$

where  $B_s(t, u)$  contains the finite (in the large- $t$  limit)  $s$ -contributions. Rather than thinking of calculating  $Z$  in the denominator we should use an experimental result on the two-point

---

<sup>7</sup>It is instructive to verify the statements made in this general discussion explicitly for the full crossover function in  $\phi^3$  theory presented in ref. [8].

scattering amplitude at some value of  $t$  for fixed  $s$  to determine it. We shall see this more explicitly below. Thus we see it is possible using the RG to produce signatured amplitudes as in (16). In the present case as we are dealing with identical bosons only positive signature states enter. Note that in the above we are only considering the leading Regge trajectory associated with the tree level value ( $g_B \rightarrow 0$ )  $\alpha = -1$ . There are, as mentioned, subleading trajectories associated with  $\alpha = -n$ ,  $n > 1$ . One can in fact regard them as corrections to the dominant scaling given by the leading Regge trajectory. In principle the RG techniques we develop here are capable of accessing these ‘‘correction to scaling’’ trajectories as well. The problem of achieving it is the rather technical one of being able to project out from the Feynman diagrams the contributions of  $O(t^{-n})$  and their associated logarithms. This can be done by analysing the Mellin transforms of the diagrams. We will not consider the matter further in this paper however.

It should be clear that our renormalization is completely crossing symmetric. If we consider the limit  $s \rightarrow \infty$  at fixed  $t$  one identifies the function  $B_s(s, t)$  such that it contains large logarithms of the type  $\ln(-s)$  which will subsequently require a multiplicative renormalization. Similarly, the function  $B_u(t, u)$ , this time in distinction to the function  $B_t(s, u)$ , will contain large logarithms of the type  $\ln s$ . A renormalization procedure totally analogous to the above will yield

$$\tilde{\Gamma}_B^{\phi\phi\phi\phi}(s, t) = \frac{g^2(s)}{-\kappa} \frac{G(t)(1 + e^{i\pi\alpha(t)})}{Z(t, g(\kappa), m(\kappa), \kappa)} \left(\frac{s}{\kappa}\right)^{\alpha(t)} + B_t(s, u). \quad (47)$$

The procedure is identical in the large- $u$  limit. Naturally in the different asymptotic limits the diagrams that contribute to the renormalization are different. For instance, a three-rung ladder diagram in the  $s$ -direction in the large- $s$  limit  $\sim g_B^6 s^{-2} K'(t) \ln s$ , whereas in the large- $t$  limit it is  $\sim g_B^6 t^{-1} K^2(s) (\ln t)^2$ . On the contrary a three-rung ladder in the  $t$ -direction varies asymptotically as  $\sim g_B^6 s^{-1} K^2(t) (\ln s)^2$  for large  $s$  and as  $\sim g_B^6 t^{-2} K'(s) K'(s) \ln t$  for large  $t$ . Thus a three-rung  $s$ -ladder contributes to the leading Regge trajectory in the large- $t$  limit but to a subleading trajectory in the large- $s$  limit. Renormalization then is capable of accessing the dual asymptotic limits,  $t \rightarrow \infty$  and  $s \rightarrow \infty$ , characteristic of the Veneziano formula and string-like behaviour.

To calculate explicitly to one loop the scattering amplitude one needs to fix the renormalization constant  $Z_t$  by choosing a normalization condition. We choose

$$B_t(s, t = \kappa, g_B, m, \kappa) = \frac{g_B^2}{-\kappa}. \quad (48)$$

The motivation for a normalization condition of this type is that in the large- $t$  limit the right hand side of (48) is what one would expect when there are no quantum fluctuations. Hence, as we will see, by this choice all fluctuations in the large- $t$  limit will be absorbed into the renormalization factor  $Z_t$  which the RG will then exponentiate. It is thus an optimum condition in terms of obtaining the maximum amount of non-perturbative information in the large- $t$  limit. We renormalize the mass as in (31), now for  $\tilde{\Gamma}_B^{\phi\phi}$ . Note that we have chosen not to implement a coupling constant renormalization.

At one loop, the large- $t$  limit of  $B_{B,t}$  is as given in (36), where we have to interpret the  $-t$  as  $e^{-i\pi}t$ , because the continuation from  $t$  on the upper edge of the threshold cut to  $e^{i\pi}t$  in

the Euclidean region has to yield a real function there (for  $s < 0$ ). With the normalization condition (48) one finds for large  $t$  and  $\kappa$

$$Z_t(s, \kappa) = 1 - g_B^2 K(s) \ln(e^{-i\pi} \kappa), \quad (49)$$

hence

$$\gamma_t(s) = -g_B^2 K(s). \quad (50)$$

Using the normalization condition again, the result for  $B_t$  is

$$B_t(s, t, g_B, m, \kappa) = \frac{g_B^2}{-\kappa} \left(\frac{t}{\kappa}\right)^{\alpha(s)}, \quad (51)$$

where the Regge trajectory,  $\alpha(s)$ , is given by

$$\alpha(s) = g_B^2 K(s) - 1. \quad (52)$$

Let us comment here briefly on terms like  $\ln t$ , where the argument of the logarithm is dimensionful: In principle such terms should be replaced by  $\ln(t/d)$  and the like, where  $d$  will in general be a function of  $s$ . For example, in (36) the function  $d$  could be determined systematically by extracting the term  $\sim t^{-1}$  in the large- $t$  expansion of the box diagram. However, for asymptotic values of  $t$  this function plays no role, and in fact it drops out when taking the derivative of  $Z_t$  with respect to  $\ln \kappa$  and hence does not appear in the renormalization group equation (40) for  $B_t$  at all. It is still present in the formal expression for  $Z_t$ .

As for the  $u$ -contributions, we can take the perturbative expression (38) with  $t = e^{-i\pi} u$  and proceed as above replacing  $t$  by  $u$  everywhere. The corresponding normalization condition reads

$$B_u(s, u = \kappa, g_B, m, \kappa) = \frac{g_B^2}{-\kappa}. \quad (53)$$

Then clearly  $Z_u = Z_t$ , and in particular we find the same expression for the Regge trajectory. We then have to continue from  $u$  on the upper edge of the  $u$ -threshold cut to  $u = e^{i\pi} t$ , giving the correct phase factor for the  $u$ -contributions, cf. (21). Note that a different prescription to determine the  $u$ -contributions would have led to  $Z_u \neq Z_t$ , so that the phase factor would have been hidden in the (undetermined) ratio  $Z_u/Z_t$ . The final result for  $\phi^3$  theory in the large- $t$  limit is

$$\tilde{\Gamma}_B^{\phi\phi\phi\phi}(s, t) = \frac{g_B^2}{-\kappa} \frac{1 + e^{i\pi\alpha(s)}}{Z(s, \kappa)} \left(\frac{t}{\kappa}\right)^{\alpha(s)} + \frac{g_B^2}{m^2 - s}. \quad (54)$$

Only the function  $Z(s, \kappa)$  in the above is not perturbatively well defined. Within the normal ‘‘philosophy’’ of renormalization this means that one has to measure the two-point scattering amplitude at a fiducial scale for  $t$  and at a fixed value of  $s$ . This will fix the value of  $Z$  for that value of  $s$ . The two-point scattering amplitude is then explicitly calculable for all other



values of  $t$ . If one wishes to know what happens at another value of  $s$  then an appropriate experiment must be carried out at that value of  $s$  for a fiducial value of  $t$ , whereupon once again one can calculate the amplitude at all other asymptotic values of  $t$ . Note that here a one-parameter family of “initial conditions”, as functions of  $s$ , must be supplied for the RG. This could be circumvented by implementing two RGs: one associated with  $t$  and another with  $s$ . In this way only one initial condition at fixed, fiducial values of both  $s$  and  $t$  would be needed. Such multiple RGs have been advocated for similar reasons in other circumstances [19]. Throughout the rest of the paper we will leave the  $Z$  factors explicit in our final formulas with the proviso that a set of experiments can be used to fix them thus leaving expressions for the scattering amplitudes which consist of explicitly calculated quantities.

For  $s = 0$  one finds the Regge intercept  $\alpha(0) = -1 + g_B^2/(16\pi^2 m^2)$ . For  $g_B^2 > 32\pi^2 m^2$  the resulting cross-section will violate the Froissart bound. This has been taken to be a serious defect of “ $s$ -channel” approaches [20]. However, at two loops just by dimensional analysis one can see that a contribution to the Regge trajectory of the form  $g_B^4/m^4$  will arise. Clearly the unitarity violating region is beyond the reach of perturbation theory. An analysis of this region requires a further renormalization — of the Regge trajectory itself. After this second renormalization  $\alpha(0)$  may continue to violate the unitarity bound. However,  $\alpha(0) > 0$  implies that  $\alpha(s) = 0$  at a negative value of  $s$  corresponding to a tachyonic “bound state”. This indicates the presence of a vacuum condensate necessitating a shift of the perturbative to the true vacuum of the theory. We will not pursue this interesting matter further here.

## 4 Matrix Renormalization

In more complicated cases than a pure  $\phi^3$  theory a pure multiplicative renormalization is not sufficient due to the mixing in the large- $t$  limit of the effective quartic interactions with different  $ijkl$ . For instance, for a theory with interactions of the form  $\phi^\dagger\phi\psi$ , where  $\phi$  is a charged scalar field and  $\psi$  a neutral one, this mixing occurs among all effective interactions in the same charge sector, i.e. there is a superselection rule preventing mixing between different sectors. Therefore we introduce a matrix multiplicative renormalization within each sector of definite charge. Considering again the limit  $t \rightarrow \infty$ , the sectors are to be taken with respect to the  $s$ -channel process, i.e. mixing occurs between pairs of particles  $(ij)$  and  $(kl)$  with the same total charge. The multiplicative renormalization of  $B_{B,t}^{ijkl}$  then takes the form

$$B_t^{ijkl}(s, t, g(\kappa), m(\kappa), \kappa) = \sum_{m,n} Z_t^{ijmn} B_{B,t}^{mnkl}(s, t, g_B, m_B, \Lambda). \quad (55)$$

We will write this and similar equations in the following in matrix form, considering  $B_t^{ijkl}$  as the entry in row  $(ij)$  and column  $(kl)$  of a matrix  $\mathbf{B}_t$ . For example, in the charge zero sector of the above bosonic theory the indices are  $(\phi^\dagger\phi)$ ,  $(\phi\phi^\dagger)$  and  $(\psi\psi)$ . Eq. (55) becomes

$$\mathbf{B}_t(s, t, g(\kappa), m(\kappa), \kappa) = \mathbf{Z}_t \mathbf{B}_{B,t}(s, t, g_B, m_B, \Lambda). \quad (56)$$

As in the  $\phi^3$  case, the  $\kappa$ -independence of  $\mathbf{B}_{B,t}$  leads to the RG equation

$$\kappa \frac{d}{d\kappa} \mathbf{B}_t(s, t, g(\kappa), m(\kappa), \kappa) = \gamma_t \mathbf{B}_t(s, t, g(\kappa), m(\kappa), \kappa), \quad (57)$$

where

$$\boldsymbol{\gamma}_t = \frac{d\mathbf{Z}_t}{d\ln\kappa} \mathbf{Z}_t^{-1}. \quad (58)$$

The normalization condition should be so chosen that  $\mathbf{Z}_t$  has an inverse.

Eq. (57) can be considered as a set of independent equations for the columns  $\mathbf{b}_t^{(i)}$  of  $\mathbf{B}_t$ . The standard way of solution then proceeds by decomposing each column into eigenvectors of  $\boldsymbol{\gamma}_t$  (we will not indicate explicitly the dependences on  $g(\kappa)$  or  $m(\kappa)$  in the following),

$$\mathbf{b}_t^{(i)}(s, t, \kappa) = \sum_j \beta_j^{(i)}(s, t, \kappa) \mathbf{v}_j(s), \quad (59)$$

where  $\mathbf{v}_j$  denotes the eigenvectors. The corresponding eigenvalues  $\gamma_j$  play the role of the “scalar”  $\gamma_t$  in the  $\phi^3$  case and determine the Regge trajectories. There seems to be no simple argument to guarantee that  $\boldsymbol{\gamma}_t$  can always be diagonalized, although we have found it to be so in all the theories considered so far. If  $\boldsymbol{\gamma}_t$  should fail to be diagonalizable, then the solution of the RG equation will typically involve logarithms of  $t$ , an interesting prospect at least.

In the remainder of this section, we will pursue the formal solution of (57) somewhat further to establish several general features of the results to one loop. In the large- $t$  limit, one-loop perturbation theory gives an expression of the form

$$\mathbf{B}_{B,t}(s, t) = \frac{g_B^2}{-t} \mathbf{b}_0 + g_B^4 \frac{\ln(e^{-i\pi}t)}{-t} \mathbf{b}_1(s), \quad (60)$$

where  $\mathbf{b}_0$  and  $\mathbf{b}_1(s)$  arise from the tree and one-loop contributions, respectively. Typical entries are 1 for  $\mathbf{b}_0$  and  $K(s)$ , as in (37), for  $\mathbf{b}_1(s)$ . As a consequence of the time reflection invariance of the bosonic theory, both matrices are symmetric.

The normalization condition

$$\mathbf{B}_t(s, t = \kappa, \kappa) = \frac{g_B^2}{-\kappa} \mathbf{b}_0 \quad (61)$$

leads to

$$\mathbf{Z}_t(s, \kappa) = 1 - g_B^2 \mathbf{b}_1(s) \mathbf{b}_0^{-1} \ln(e^{-i\pi}\kappa), \quad (62)$$

so the RG equation reads

$$\kappa \frac{d}{d\kappa} \mathbf{B}_t(s, t, \kappa) = \boldsymbol{\gamma}_t(s) \mathbf{B}_t(s, t, \kappa) \quad (63)$$

with

$$\boldsymbol{\gamma}_t(s) = -g_B^2 \mathbf{b}_1(s) \mathbf{b}_0^{-1}. \quad (64)$$

Of course, for the formalism to work,  $\mathbf{b}_0$  has to be invertible.

Solving the RG equation yields, by use of the normalization condition (61),

$$\begin{aligned}\mathbf{B}_t(s, t, \kappa) &= \exp\left(-\gamma_t(s) \ln \frac{t}{\kappa}\right) \mathbf{B}_t(s, t, t) \\ &= \frac{g_B^2}{-t} \sum_{k=0}^{\infty} \frac{g_B^{2k}}{k!} \left(\ln \frac{t}{\kappa}\right)^k (\mathbf{b}_1(s) \mathbf{b}_0^{-1})^k \mathbf{b}_0.\end{aligned}\quad (65)$$

From the last form it is obvious that  $\mathbf{B}_t$  is again a symmetric matrix, as it should be. Invoking the decomposition (59) of the columns of  $\mathbf{B}_t$  into eigenvectors of  $\gamma_t$ , (65) can be written in the form ( $\gamma_j$  are the eigenvalues of  $\gamma_t$ )

$$\mathbf{b}_t^{(i)}(s, t, \kappa) = \sum_j \beta_j^{(i)}(s, t, t) \left(\frac{t}{\kappa}\right)^{-\gamma_j(s)} \mathbf{v}_j(s), \quad (66)$$

where the integration constants at  $\kappa = t$  are fixed by (61) in the following way:

$$\frac{g_B^2}{-t} \mathbf{b}_0^{(i)} = \sum_j \beta_j^{(i)}(s, t, t) \mathbf{v}_j(s), \quad (67)$$

$\mathbf{b}_0^{(i)}$  being the  $i$ -th column of  $\mathbf{b}_0$ .

We now come to the  $u$ -contributions. In the large- $u$  limit one finds

$$\mathbf{B}_{B,u}(s, u) = \frac{g_B^2}{-u} \mathbf{b}'_0 + g_B^4 \frac{\ln(e^{-i\pi}u)}{-u} \mathbf{b}'_1(s), \quad (68)$$

where the matrices  $\mathbf{b}'_0, \mathbf{b}'_1$  are related to  $\mathbf{b}_0, \mathbf{b}_1$  by crossing symmetry. More precisely, the  $u$ -contribution diagrams are obtained from the corresponding  $t$ -contribution ones by interchanging the incoming particles. For the matrices this implies interchanging columns, for example the ones with indices  $(\phi\phi^\dagger)$  and  $(\phi^\dagger\phi)$ . We can write this formally as

$$\mathbf{b}'_0 = \mathbf{b}_0 S, \quad \mathbf{b}'_1(s) = \mathbf{b}_1(s) S \quad (69)$$

with a permutation matrix  $S$ . Alternatively, we could interchange the outgoing particles, corresponding to interchanging rows of the matrices. This implies the following property of  $\mathbf{b}_0$  and  $\mathbf{b}_1$ :

$$S \mathbf{b}_0 = \mathbf{b}_0 S, \quad S \mathbf{b}_1(s) = \mathbf{b}_1(s) S. \quad (70)$$

We use as normalization condition for the  $u$ -contributions that

$$\mathbf{B}_u(s, u = \kappa, \kappa) = \frac{g_B^2}{-\kappa} \mathbf{b}'_0. \quad (71)$$

Now (69) implies

$$\mathbf{b}'_1(s) \mathbf{b}'_0{}^{-1} = \mathbf{b}_1(s) \mathbf{b}_0^{-1}, \quad (72)$$

and hence that  $\mathbf{Z}_u = \mathbf{Z}_t$  and  $\gamma_u = \gamma_t$ . In particular, the Regge trajectories are the same as for the  $t$ -contributions.

To see the appearance of signatures in the general case property (70), arising from crossing symmetry, plays a crucial role. We first deduce, using  $S = S^{-1}$ , that

$$S \gamma_t(s) = \gamma_t(s) S, \quad (73)$$

i.e.  $\gamma_t$  commutes with  $S$ . Assuming for the moment that the eigenvalues of  $\gamma_t$  are non-degenerate, we conclude that the eigenvectors satisfy

$$S \mathbf{v}_j(s) = \sigma_j \mathbf{v}_j(s) \quad (74)$$

and, because  $S^2 = 1$ , we have  $\sigma_j = \pm 1$ . In the degenerate case we can always, by application of the projection operators

$$\Sigma_{\pm} = \frac{1 \pm S}{2}, \quad (75)$$

select a basis of the eigenspace consisting of eigenvectors with definite ‘signature’ as in (74). Applying this to the decomposition of the  $u$ -contributions at  $\kappa = t$  corresponding to (67),

$$\frac{g_B^2}{-u} \mathbf{b}_0^{(i)} = \frac{g_B^2}{-u} S \mathbf{b}_0^{(i)} = \sum_j \sigma_j \beta_j^{(i)}(s, u, u) \mathbf{v}_j(s), \quad (76)$$

we obtain for the coefficients of the  $u$ -contributions

$$\beta_j^{(i)}(s, u, u) = \sigma_j \beta_j^{(i)}(s, u, u). \quad (77)$$

Consequently, the sum of  $\mathbf{B}_t$  and  $\mathbf{B}_u$  is of the form (by columns)

$$\begin{aligned} & \mathbf{b}_t^{(i)}(s, t, \kappa) + \mathbf{b}_u^{(i)}(s, u, \kappa) \\ &= \sum_j \left[ \beta_j^{(i)}(s, t, t) \left(\frac{t}{\kappa}\right)^{-\gamma_j(s)} + \sigma_j \beta_j^{(i)}(s, u, u) \left(\frac{u}{\kappa}\right)^{-\gamma_j(s)} \right] \mathbf{v}_j(s), \end{aligned} \quad (78)$$

featuring the signatures  $\sigma_j$ . This demonstration also shows the link between the signatures of the Regge trajectories and the symmetry properties of the eigenvectors of  $\gamma_t$ .

Let us finally comment on the effect of the factor  $\mathbf{Z}_t^{-1}$  necessary to convert  $\mathbf{B}_t$  to the bare quantity  $\mathbf{B}_{B,t}$ . By virtue of (62) and (64) we have

$$\mathbf{Z}_t^{-1}(s, \kappa) = 1 - \ln(e^{-i\pi} \kappa) \gamma_t, \quad (79)$$

so that the application to (66) gives, for example,

$$\begin{aligned} \mathbf{b}_{B,t}^{(i)}(s, t) &= \mathbf{Z}_t^{-1}(s, \kappa) \mathbf{b}_t^{(i)}(s, t, \kappa) \\ &= \sum_j \left( 1 - \ln(e^{-i\pi} \kappa) \gamma_j \right) \beta_j^{(i)}(s, t, t) \left(\frac{t}{\kappa}\right)^{-\gamma_j(s)} \mathbf{v}_j(s), \end{aligned} \quad (80)$$

an analogous formula holding for the  $u$ -contributions. We conclude that the amplitude of each Regge trajectory gets modified by a certain function  $Z_j^{-1}(s, \kappa)$  which, however, is the same for all contributions to one and the same trajectory. In particular, the  $t$ - and  $u$ -contributions to a single trajectory get modified by the same function, hence signature is preserved. The same argument applies if  $\mathbf{Z}_t$  is an arbitrary power series in  $\gamma_t$  (as far as the matrix structure is concerned), so although the expression for  $\mathbf{Z}_t$  is formal, it appears reasonable to assume that the argument continues to hold for the “true”  $\mathbf{Z}_t$  to the present approximation.

To summarize, we have developed a renormalization scheme that reproduces from perturbation theory the predictions of Regge theory. It has proved necessary to introduce several non-standard ideas in the renormalization program. In order to fully justify the renormalization scheme presented we have to demonstrate that it can be extended to higher orders, and that the one-loop renormalization group improved result sums the leading logs to all orders in perturbation theory. We will demonstrate in appendix A the consistency of the scheme to two loops, while in appendix B we show that the one-loop renormalization sums the leading logs completely. In the next section we will present explicit results for the case of  $\phi^\dagger\phi\psi$  theory.

## 5 Application to $\phi^\dagger\phi\psi$ Theory

In this section we apply the above method to the case of a bosonic theory with a charged scalar field  $\phi$  and a neutral scalar field  $\psi$ , interacting through a cubic coupling  $\phi^\dagger\phi\psi$ . We denote the masses of the  $\phi$  and  $\psi$  particles as  $m$  and  $M$ , respectively. They will be renormalized on mass shell as in (31). We do not implement a renormalization for the coupling constant  $g_B$ .

Let us consider the large- $t$  limit and begin with the charge  $Q = +1$  sector. To illustrate the method described in the last two sections we will explain this case in full detail. The possible pairs of particles corresponding to this charge are  $(\phi\psi)$  and  $(\psi\phi)$  (taking the charge of the  $\phi$ -particle equal to one). Consequently, we have to consider  $2 \times 2$  matrices with indices  $(\phi\psi)$  and  $(\psi\phi)$  to take into account the mixing of effective couplings. To one loop, perturbation theory gives for the matrix of  $t$ -contributions

$$\mathbf{B}_{B,t}(s, t) = \left( \begin{array}{cc} \text{Diagram 1} & \text{Diagram 2} \\ \text{Diagram 3} & \text{Diagram 4} \end{array} \right) \xrightarrow{t \rightarrow \infty} \left( \begin{array}{cc} \text{Diagram 5} & \text{Diagram 6} \\ \text{Diagram 7} & \text{Diagram 8} \end{array} \right). \quad (81)$$

Let us consider the contraction of the “d-lines” (the horizontal propagators in this case) in the large- $t$  limit in more detail: We have

$$\mathbf{B}_{B,t}^{\phi\psi\psi\phi}(s, t) = \text{Diagram 9} \xrightarrow{t \rightarrow \infty} \text{Diagram 10} \equiv \frac{g_B^2}{-t},$$

$$\begin{aligned}
\mathbf{B}_{B,t}^{\psi\phi\phi\psi}(s,t) &= \text{diagram} \xrightarrow{t \rightarrow \infty} \text{diagram} \equiv \frac{g_B^2}{-t}, \\
\mathbf{B}_{B,t}^{\phi\psi\phi\psi}(s,t) &= \text{diagram} \xrightarrow{t \rightarrow \infty} \text{diagram} \equiv g_B^4 \frac{\ln(-t)}{-t} K_{Mm}(s), \\
\mathbf{B}_{B,t}^{\psi\phi\psi\phi}(s,t) &= \text{diagram} \xrightarrow{t \rightarrow \infty} \text{diagram} \equiv g_B^4 \frac{\ln(-t)}{-t} K_{Mm}(s), \quad (82)
\end{aligned}$$

where the one-loop diagrams show the characteristic and important factorization property in the limit  $t \gg s, m^2, M^2$ . The function  $K_{Mm}(s)$  is a *two-dimensional* one-loop diagram, showing that the effective degrees of freedom in this limit are different from those at  $t \sim s$ . One can immediately see this by calculating the box diagram using the standard Feynman parameterization trick. Consider as an illustration the simpler diagram

$$\begin{aligned}
\text{diagram} &\equiv \frac{g_B^4}{(4\pi)^2} \int_0^1 \frac{d\alpha_1 d\alpha_2 d\beta_1 d\beta_2 \delta(1 - \alpha_1 - \alpha_2 - \beta_1 - \beta_2)}{[-\alpha_1 \alpha_2 t + (\alpha_1 + \alpha_2) M^2 + (\beta_1 + \beta_2)^2 m^2 - \beta_1 \beta_2 s]^2} \\
&\xrightarrow{t \rightarrow \infty} \frac{g_B^4}{(4\pi)^2} \int_0^1 d\beta_1 d\beta_2 \delta(1 - \beta_1 - \beta_2) \int_0^\epsilon \frac{d\alpha_1 d\alpha_2}{[-\alpha_1 \alpha_2 t + (\beta_1 + \beta_2)^2 m^2 - \beta_1 \beta_2 s]^2} \\
&= \left\{ \frac{g_B^4}{(4\pi)^2} \int_0^1 \frac{d\beta_1 d\beta_2 \delta(1 - \beta_1 - \beta_2)}{(\beta_1 + \beta_2)^2 m^2 - \beta_1 \beta_2 s} \right\} \frac{\ln(-t)}{-t} \\
&= g_B^4 \frac{\ln(-t)}{-t} K_m(s) \equiv \text{diagram} \quad (83)
\end{aligned}$$

where in taking the limit  $t \rightarrow \infty$  only the “end point region”  $\alpha_1 \simeq \alpha_2 \simeq 0$  has been considered, and from the second to the third line contributions of  $O(t^{-1})$  have been neglected. The expression in curly brackets is the integral corresponding to the two-dimensional one-loop contracted diagram  $K_m(s)$  as shown above. Note that in our notation the graphs include the factor  $\ln(-t)/(-t)$  as well as the couplings  $g_B$  appearing at each vertex. Observe in particular that by taking the limit the dependence on the mass  $M$  of the exchanged particle has disappeared.

The function  $K_m(s)$  coincides with the  $K(s)$  defined in (37). In the slightly more complicated case where the two-dimensional propagators have different masses, we get

$$\begin{aligned}
K_{Mm}(s) &= \frac{1}{16\pi^2} \int_0^1 \frac{d\beta}{\beta M^2 + (1 - \beta)m^2 - \beta(1 - \beta)s} \\
&= \frac{1}{4\pi^2} \frac{\arctan\left(\frac{s - (M - m)^2}{(M + m)^2 - s}\right)^{\frac{1}{2}}}{[(s - (M - m)^2)((M + m)^2 - s)]^{\frac{1}{2}}} \quad (84)
\end{aligned}$$

for  $s < (M + m)^2$ . For  $M = m$  this formula reduces to the one for  $K_m(s)$ .

From (82) the matrix  $\mathbf{B}_{B,t}$  is given by

$$\mathbf{B}_{B,t}(s, t) = \frac{g_B^2}{-t} \begin{pmatrix} g_B^2 K_{Mm}(s) \ln(e^{-i\pi} t) & 1 \\ 1 & g_B^2 K_{Mm}(s) \ln(e^{-i\pi} t) \end{pmatrix}, \quad (85)$$

where  $-t$  has been taken as  $e^{-i\pi} t$  corresponding to  $t$  lying on the upper (“physical”) edge of the threshold cut. We use the normalization condition

$$\mathbf{B}_t(s, t = \kappa, \kappa) = \frac{g_B^2}{-\kappa} \begin{pmatrix} 0 & 1 \\ 1 & 0 \end{pmatrix}. \quad (86)$$

corresponding to the tree contributions, with the motivation that we wish to absorb as much as possible of the quantum fluctuations into the renormalization constant. Then  $\mathbf{B}_t = \mathbf{Z}_t \mathbf{B}_{B,t}$  implies

$$\mathbf{Z}_t(s, \kappa) = \begin{pmatrix} 1 & -g_B^2 K_{Mm}(s) \ln(e^{-i\pi} \kappa) \\ -g_B^2 K_{Mm}(s) \ln(e^{-i\pi} \kappa) & 1 \end{pmatrix}, \quad (87)$$

neglecting terms of  $O(g_B^4)$ . Hence

$$\boldsymbol{\gamma}_t(s) = \frac{d\mathbf{Z}_t}{d \ln \kappa} \mathbf{Z}_t^{-1} = \begin{pmatrix} 0 & -g_B^2 K_{Mm}(s) \\ -g_B^2 K_{Mm}(s) & 0 \end{pmatrix}. \quad (88)$$

To solve the RG equation

$$\kappa \frac{d}{d\kappa} \mathbf{B}_t(s, t, \kappa) = \boldsymbol{\gamma}_t(s) \mathbf{B}_t(s, t, \kappa), \quad (89)$$

we consider it as a set of two equations for the columns  $\mathbf{b}_t^{(i)}$  of the matrix  $\mathbf{B}_t$ . Each column will be expressed as a linear combination of the (two) independent eigenvectors of  $\boldsymbol{\gamma}_t$ ,

$$\mathbf{b}_t^{(i)}(s, t, \kappa) = \beta_+^{(i)}(s, t, \kappa) \mathbf{v}_+(s) + \beta_-^{(i)}(s, t, \kappa) \mathbf{v}_-(s). \quad (90)$$

The eigenvectors and corresponding eigenvalues of  $\boldsymbol{\gamma}_t$  are given by

$$\begin{aligned} \mathbf{v}_+ &= \begin{pmatrix} 1 \\ 1 \end{pmatrix}, & \gamma_+(s) &= -g_B^2 K_{Mm}(s), \\ \mathbf{v}_- &= \begin{pmatrix} -1 \\ 1 \end{pmatrix}, & \gamma_-(s) &= g_B^2 K_{Mm}(s). \end{aligned} \quad (91)$$

Eq. (89) now becomes a set of four independent differential equations for the coefficients  $\beta_{\pm}^{(i)}$ ,

$$\frac{d}{d \ln \kappa} \beta_{\pm}^{(i)}(s, t, \kappa) = \gamma_{\pm}(s) \beta_{\pm}^{(i)}(s, t, \kappa). \quad (92)$$

The integration of these equations (from  $t$  to  $\kappa$ ) immediately reveals the Regge behaviour:

$$\beta_{\pm}^{(i)}(s, t, \kappa) = \beta_{\pm}^{(i)}(s, t, t) \left( \frac{t}{\kappa} \right)^{-\gamma_{\pm}(s)}. \quad (93)$$

The normalization condition (86) fixes the integration constants  $\beta_{\pm}^{(i)}(s, t, t)$ . The final result for the  $t$ -contributions is

$$\mathbf{B}_t(s, t, \kappa) = \frac{g_B^2}{-2\kappa} \begin{pmatrix} \left(\frac{t}{\kappa}\right)^{\alpha_+(s)} - \left(\frac{t}{\kappa}\right)^{\alpha_-(s)} & \left(\frac{t}{\kappa}\right)^{\alpha_+(s)} + \left(\frac{t}{\kappa}\right)^{\alpha_-(s)} \\ \left(\frac{t}{\kappa}\right)^{\alpha_+(s)} + \left(\frac{t}{\kappa}\right)^{\alpha_-(s)} & \left(\frac{t}{\kappa}\right)^{\alpha_+(s)} - \left(\frac{t}{\kappa}\right)^{\alpha_-(s)} \end{pmatrix} \quad (94)$$

with the Regge trajectories

$$\alpha_{\pm}(s) = -\gamma_{\pm}(s) - 1 = \pm g_B^2 K_{Mm}(s) - 1. \quad (95)$$

We can repeat the same procedure for the  $u$ -contributions, considering this time the large- $u$  limit. The corresponding matrix  $\mathbf{B}_{B,u}$  from one-loop perturbation theory reads

$$\mathbf{B}_{B,u}(s, u) = \left( \begin{array}{cc} \text{Diagram 1} & \text{Diagram 2} \\ \text{Diagram 3} & \text{Diagram 4} \end{array} \right) \xrightarrow{u \rightarrow \infty} \left( \begin{array}{cc} \text{Diagram 5} & \text{Diagram 6} \\ \text{Diagram 7} & \text{Diagram 8} \end{array} \right), \quad (96)$$

implying

$$\mathbf{B}_u(s, u) = \frac{g_B^2}{-u} \begin{pmatrix} 1 & g_B^2 K_{Mm}(s) \ln(e^{-i\pi} u) \\ g_B^2 K_{Mm}(s) \ln(e^{-i\pi} u) & 1 \end{pmatrix}. \quad (97)$$

The computation is identical to (83), just replacing  $t$  by  $u$ . Imposing the analogous normalization condition

$$\mathbf{B}_u(s, u = \kappa, \kappa) = \frac{g_B^2}{-\kappa} \begin{pmatrix} 1 & 0 \\ 0 & 1 \end{pmatrix} \quad (98)$$

leads to the expected result that  $\mathbf{Z}_u = \mathbf{Z}_t$  and  $\gamma_u = \gamma_t$ , hence the RG equation for  $\mathbf{B}_u$  is the same as that for the  $t$ -contributions. However, the columns in the normalization condition are interchanged, so that finally

$$\mathbf{B}_u(s, u, \kappa) = \frac{g_B^2}{-2\kappa} \begin{pmatrix} \left(\frac{u}{\kappa}\right)^{\alpha_+(s)} + \left(\frac{u}{\kappa}\right)^{\alpha_-(s)} & \left(\frac{u}{\kappa}\right)^{\alpha_+(s)} - \left(\frac{u}{\kappa}\right)^{\alpha_-(s)} \\ \left(\frac{u}{\kappa}\right)^{\alpha_+(s)} - \left(\frac{u}{\kappa}\right)^{\alpha_-(s)} & \left(\frac{u}{\kappa}\right)^{\alpha_+(s)} + \left(\frac{u}{\kappa}\right)^{\alpha_-(s)} \end{pmatrix} \quad (99)$$

with the same Regge trajectories as above. The analytic continuation to  $u = -t$ , as explained in the last section, amounts to replacing  $u$  by  $e^{i\pi} t$ .

The  $s$ -contributions at tree level are independent of  $t$  and read

$$\mathbf{B}_s(s) = \left( \begin{array}{cc} \text{Diagram 9} & \text{Diagram 10} \\ \text{Diagram 11} & \text{Diagram 12} \end{array} \right) = \frac{g_B^2}{m^2 - s} \begin{pmatrix} 1 & 1 \\ 1 & 1 \end{pmatrix}. \quad (100)$$



The corresponding two-particle scattering amplitudes  $\tilde{\Gamma}_B^{ijkl}$  are then given by the matrix

$$\tilde{\Gamma}_B(s, t) = \mathbf{B}_s(s) + \mathbf{Z}^{-1}(s, \kappa) (\mathbf{B}_t(s, t, \kappa) + \mathbf{B}_u(s, t, \kappa)) . \quad (101)$$

Taking the formal expression for  $\mathbf{Z} = \mathbf{Z}_t$  from (87), we have

$$\mathbf{Z}^{-1}(s, \kappa) \mathbf{v}_\pm = \left( \mathbf{1} - \ln(e^{-i\pi} \kappa) \boldsymbol{\gamma}_t(s) \right) \mathbf{v}_\pm = \left( 1 \pm g_B^2 K_{Mm}(s) \ln(e^{-i\pi} \kappa) \right) \mathbf{v}_\pm . \quad (102)$$

As discussed in the last section we assume that the “true”  $\mathbf{Z}^{-1}$  acts similarly, leading to the same functions of  $s$  and  $\kappa$  for all contributions corresponding to the same eigenvector and hence to the same Regge trajectory. The final result for the charge one sector is then

$$\begin{aligned} \tilde{\Gamma}_B^{\phi\psi\phi\psi}(s, t) &= \tilde{\Gamma}_B^{\psi\phi\psi\phi}(s, t) \\ &= \frac{g_B^2}{m^2 - s} - \frac{g_B^2}{2\kappa} \frac{1 + e^{i\pi\alpha_+(s)}}{Z_+(s, \kappa)} \left( \frac{t}{\kappa} \right)^{\alpha_+(s)} + \frac{g_B^2}{2\kappa} \frac{1 - e^{i\pi\alpha_-(s)}}{Z_-(s, \kappa)} \left( \frac{t}{\kappa} \right)^{\alpha_-(s)} , \end{aligned} \quad (103)$$

$$\begin{aligned} \tilde{\Gamma}_B^{\phi\psi\psi\phi}(s, t) &= \tilde{\Gamma}_B^{\psi\phi\phi\psi}(s, t) \\ &= \frac{g_B^2}{m^2 - s} - \frac{g_B^2}{2\kappa} \frac{1 + e^{i\pi\alpha_+(s)}}{Z_+(s, \kappa)} \left( \frac{t}{\kappa} \right)^{\alpha_+(s)} - \frac{g_B^2}{2\kappa} \frac{1 - e^{i\pi\alpha_-(s)}}{Z_-(s, \kappa)} \left( \frac{t}{\kappa} \right)^{\alpha_-(s)} . \end{aligned} \quad (104)$$

We should think of the  $s$ -dependent factors  $Z_+$  and  $Z_-$  as fixed by experiment, for example by measuring the functions  $\tilde{\Gamma}_B^{\phi\psi\phi\psi}$  and  $\tilde{\Gamma}_B^{\phi\psi\psi\phi}$  at some fiducial value  $t = \kappa$ .

All the general properties demonstrated in the last section can be verified explicitly for this example, as for instance the symmetry properties of the emerging matrices. In particular, we see how the signature of the Regge trajectories is related to the symmetry of the corresponding eigenvectors under the exchange of components. Of course, an identical calculation holds for the charge  $Q = -1$  sector (just reverse the sense of the arrows in the diagrams).

Now we turn to the zero charge sector. In this case, mixing will occur between the pairs of particles  $(\phi^\dagger\phi)$ ,  $(\phi\phi^\dagger)$  and  $(\psi\psi)$ , hence the mixing matrices are  $3 \times 3$ . To one loop the  $t$ -contribution matrix has the form

$$\begin{aligned} \mathbf{B}_{B,t}(s, t) &= \frac{g_B^2}{-t} \begin{pmatrix} 1 & 0 & 1 \\ 0 & 1 & 1 \\ 1 & 1 & 0 \end{pmatrix} \\ &+ g_B^4 \frac{\ln(e^{-i\pi} t)}{-t} \begin{pmatrix} K_m(s) + K_M(s) & K_M(s) & K_m(s) \\ K_M(s) & K_m(s) + K_M(s) & K_m(s) \\ K_m(s) & K_m(s) & 2K_m(s) \end{pmatrix} \end{aligned} \quad (105)$$

in the large- $t$  limit. The corresponding diagrams, as well as several details of the following calculation, are given in appendix C. Using again a normalization condition corresponding

to the tree contributions we obtain

$$\gamma_t(s) = -g_B^2 \begin{pmatrix} K_m(s) & 0 & K_M(s) \\ 0 & K_m(s) & K_M(s) \\ K_m(s) & K_m(s) & 0 \end{pmatrix}. \quad (106)$$

Observe that  $\gamma_t$  is not symmetric, but that nevertheless

$$\gamma_t(s) S = S \gamma_t(s), \quad (107)$$

where the permutation matrix

$$S = \begin{pmatrix} 0 & 1 & 0 \\ 1 & 0 & 0 \\ 0 & 0 & 1 \end{pmatrix} \quad (108)$$

exchanges the first two rows or columns. The matrix  $\gamma_t$  possesses three linear independent eigenvectors with

$$S \mathbf{v}_\pm(s) = \mathbf{v}_\pm(s), \quad S \mathbf{v}_0(s) = -\mathbf{v}_0(s), \quad (109)$$

so that we expect the corresponding trajectories  $\alpha_\pm$  to have positive, and  $\alpha_0$  to have negative, signature.

The matrix of  $u$ -contributions can be obtained from  $\mathbf{B}_{B,t}$  by interchanging the first two rows (or columns), and replacing  $t$  by  $u$ . Let us proceed here directly to the final result for the charge zero sector, referring to appendix C for the intermediate steps. The scattering amplitudes turn out to be in the present approximation

$$\begin{aligned} \tilde{\Gamma}_B^{\phi^\dagger\phi\phi^\dagger\phi}(s,t) &= \tilde{\Gamma}_B^{\phi\phi^\dagger\phi\phi^\dagger}(s,t) = \frac{g_B^2}{M^2-s} - \frac{g_B^2}{\kappa} \frac{C_+(s)(1+e^{i\pi\alpha_+(s)})}{Z_+(s,\kappa)} \left(\frac{t}{\kappa}\right)^{\alpha_+(s)} \\ &\quad - \frac{g_B^2}{\kappa} \frac{C_-(s)(1+e^{i\pi\alpha_-(s)})}{Z_-(s,\kappa)} \left(\frac{t}{\kappa}\right)^{\alpha_-(s)} - \frac{g_B^2}{2\kappa} \frac{(1-e^{i\pi\alpha_0(s)})}{Z_0(s,\kappa)} \left(\frac{t}{\kappa}\right)^{\alpha_0(s)}, \end{aligned} \quad (110)$$

$$\begin{aligned} \tilde{\Gamma}_B^{\phi^\dagger\phi\phi\phi^\dagger}(s,t) &= \tilde{\Gamma}_B^{\phi\phi^\dagger\phi^\dagger\phi}(s,t) = \frac{g_B^2}{M^2-s} - \frac{g_B^2}{\kappa} \frac{C_+(s)(1+e^{i\pi\alpha_+(s)})}{Z_+(s,\kappa)} \left(\frac{t}{\kappa}\right)^{\alpha_+(s)} \\ &\quad - \frac{g_B^2}{\kappa} \frac{C_-(s)(1+e^{i\pi\alpha_-(s)})}{Z_-(s,\kappa)} \left(\frac{t}{\kappa}\right)^{\alpha_-(s)} + \frac{g_B^2}{2\kappa} \frac{(1-e^{i\pi\alpha_0(s)})}{Z_0(s,\kappa)} \left(\frac{t}{\kappa}\right)^{\alpha_0(s)}, \end{aligned} \quad (111)$$

$$\begin{aligned} \tilde{\Gamma}_B^{\phi^\dagger\phi\psi\psi}(s,t) &= \tilde{\Gamma}_B^{\phi\phi^\dagger\psi\psi}(s,t) = \tilde{\Gamma}_B^{\psi\psi\phi^\dagger\phi}(s,t) = \tilde{\Gamma}_B^{\psi\psi\phi\phi^\dagger}(s,t) \\ &= -\frac{g_B^2}{\kappa} \frac{D_+(s)(1+e^{i\pi\alpha_+(s)})}{Z_+(s,\kappa)} \left(\frac{t}{\kappa}\right)^{\alpha_+(s)} - \frac{g_B^2}{\kappa} \frac{D_-(s)(1+e^{i\pi\alpha_-(s)})}{Z_-(s,\kappa)} \left(\frac{t}{\kappa}\right)^{\alpha_-(s)}, \end{aligned} \quad (112)$$

$$\begin{aligned} \tilde{\Gamma}_B^{\psi\psi\psi\psi}(s, t) &= -\frac{g_B^2}{\kappa} \frac{E(s)(1 + e^{i\pi\alpha_+(s)})}{Z_+(s, \kappa)} \left(\frac{t}{\kappa}\right)^{\alpha_+(s)} + \frac{g_B^2}{\kappa} \frac{E(s)(1 + e^{i\pi\alpha_-(s)})}{Z_-(s, \kappa)} \left(\frac{t}{\kappa}\right)^{\alpha_-(s)}, \end{aligned} \quad (113)$$

where we have also included the  $s$ -contributions. The Regge trajectories with the expected signatures are explicitly

$$\begin{aligned} \alpha_{\pm}(s) &= \frac{g_B^2 K_m(s)}{2} \left( 1 \pm \left( 1 + 8 \frac{K_M(s)}{K_m(s)} \right)^{\frac{1}{2}} \right) - 1, \\ \alpha_0(s) &= g_B^2 K_m(s) - 1, \end{aligned} \quad (114)$$

and the amplitudes  $C_{\pm}$ ,  $D_{\pm}$  and  $E$  are given in the appendix. We have found a surprisingly rich structure here. Observe in particular that the negative-signature trajectory  $\alpha_0$  does not mix with  $(\psi\psi)$ -states.

The last case to be considered is the charge  $Q = 2$  sector. In this case we do not need to implement a matrix renormalization. The  $t$ -contributions are given by

$$\begin{aligned} B_{B,t}^{\phi\phi\phi\phi}(s, t) &= \text{diagram 1} + \text{diagram 2} \\ \xrightarrow{t \rightarrow \infty} & \text{diagram 3} + \text{diagram 4} \equiv \frac{g_B^2}{-t} + g_B^4 \frac{\ln(e^{-i\pi}t)}{-t} K_m(s), \end{aligned} \quad (115)$$

the same as (36) for  $\phi^3$  theory. Consequently the whole renormalization procedure is exactly the same as in section 3. For better comparison with the limit of large  $s$  to be discussed below, we also present the graphs for the  $u$ -contributions:

$$\begin{aligned} B_{B,u}^{\phi\phi\phi\phi}(s, u) &= \text{diagram 5} + \text{diagram 6} \\ \xrightarrow{u \rightarrow \infty} & \text{diagram 7} + \text{diagram 8} \equiv \frac{g_B^2}{-u} + g_B^4 \frac{\ln(e^{-i\pi}u)}{-u} K_m(s). \end{aligned} \quad (116)$$

The result for the scattering amplitude is then

$$\tilde{\Gamma}_B^{\phi\phi\phi\phi}(s, t) = \frac{g_B^2}{-\kappa} \frac{1 + e^{i\pi\alpha(s)}}{Z(s, \kappa)} \left(\frac{t}{\kappa}\right)^{\alpha(s)}, \quad \alpha(s) = g_B^2 K_m(s) - 1. \quad (117)$$

Note that there are no  $s$ -contributions here, in contradistinction to  $\phi^3$  theory. The Regge trajectory is the same as  $\alpha_0$  in the zero charge sector, the reason being the absence of mixing with  $(\psi\psi)$ -states there. As is apparent from the diagrams, we obtain identical results in the charge  $Q = -2$  sector.

We remark that our results for  $\phi^\dagger\phi\psi$  theory also apply to several similar bosonic theories. For example, the corresponding results for the Wick-Cutkosky model (for the process  $\phi_1\phi_2 \rightarrow \phi_1\phi_2$ ) can be obtained from the charge two sector of  $\phi^\dagger\phi\psi$  theory just by ignoring

the  $u$ -contributions because of the absence of exchange interactions in this case. Slightly different trajectories are obtained in a  $\phi^2\psi$  theory, where the  $\phi$ -particle is uncharged. The corresponding results are given in ref. [8].

In the above we have exclusively considered the asymptotic large- $t$  behaviour of the theory. If we are interested in the asymptotic behaviour of the two-particle on-shell scattering amplitude in the large- $s$  limit we have to consider that the mixing among the different quartic interactions has to be seen in sectors of charge according to the processes in the  $t$ -channel. For example in the charge  $Q_t = 1$  sector the mixing occurs between the following quartic interactions:

$$\begin{array}{c} t \leftarrow \\ s \uparrow \end{array} \left( \begin{array}{cc} \begin{array}{c} \text{---} \diagup \text{---} \\ \text{---} \diagdown \text{---} \\ \text{---} \diagup \text{---} \\ \text{---} \diagdown \text{---} \end{array} & \begin{array}{c} \text{---} \diagup \text{---} \\ \text{---} \diagdown \text{---} \\ \text{---} \diagup \text{---} \\ \text{---} \diagdown \text{---} \end{array} \\ \begin{array}{c} \text{---} \diagup \text{---} \\ \text{---} \diagdown \text{---} \\ \text{---} \diagup \text{---} \\ \text{---} \diagdown \text{---} \end{array} & \begin{array}{c} \text{---} \diagup \text{---} \\ \text{---} \diagdown \text{---} \\ \text{---} \diagup \text{---} \\ \text{---} \diagdown \text{---} \end{array} \end{array} \right), \quad (118)$$

where now the indices  $(\phi\psi)$  and  $(\psi\phi)$  have been arranged according to the outgoing (rows) and incoming (columns) particles in the  $t$ -channel. To coincide with the order of the indices for the matrix, the incoming particles are shown as entering the diagrams from the right.

For illustration, we present the diagrams for the simplest case of charge  $Q_t = 2$  in the large- $s$  limit. To one loop we have for the  $s$ -contributions

$$\begin{array}{c} B_{B,s}^{\phi\phi\phi\phi}(s,t) \\ \xrightarrow{s \rightarrow \infty} \end{array} = \begin{array}{c} \begin{array}{c} \text{---} \diagup \text{---} \\ \text{---} \diagdown \text{---} \\ \text{---} \diagup \text{---} \\ \text{---} \diagdown \text{---} \end{array} + \begin{array}{c} \text{---} \diagup \text{---} \\ \text{---} \diagdown \text{---} \\ \text{---} \diagup \text{---} \\ \text{---} \diagdown \text{---} \end{array} \\ \begin{array}{c} \text{---} \diagup \text{---} \\ \text{---} \diagdown \text{---} \\ \text{---} \diagup \text{---} \\ \text{---} \diagdown \text{---} \end{array} + \begin{array}{c} \text{---} \diagup \text{---} \\ \text{---} \diagdown \text{---} \\ \text{---} \diagup \text{---} \\ \text{---} \diagdown \text{---} \end{array} \end{array} \equiv \frac{g_B^2}{-s} + g_B^4 \frac{\ln(e^{-i\pi}s)}{-s} K_m(t), \quad (119)$$

while the  $u$ -contributions turn out to be

$$\begin{array}{c} B_{B,u}^{\phi\phi\phi\phi}(t,u) \\ \xrightarrow{u \rightarrow \infty} \end{array} = \begin{array}{c} \begin{array}{c} \text{---} \diagup \text{---} \\ \text{---} \diagdown \text{---} \\ \text{---} \diagup \text{---} \\ \text{---} \diagdown \text{---} \end{array} + \begin{array}{c} \text{---} \diagup \text{---} \\ \text{---} \diagdown \text{---} \\ \text{---} \diagup \text{---} \\ \text{---} \diagdown \text{---} \end{array} \\ \begin{array}{c} \text{---} \diagup \text{---} \\ \text{---} \diagdown \text{---} \\ \text{---} \diagup \text{---} \\ \text{---} \diagdown \text{---} \end{array} + \begin{array}{c} \text{---} \diagup \text{---} \\ \text{---} \diagdown \text{---} \\ \text{---} \diagup \text{---} \\ \text{---} \diagdown \text{---} \end{array} \end{array} \equiv \frac{g_B^2}{-u} + g_B^4 \frac{\ln(e^{-i\pi}u)}{-u} K_m(t). \quad (120)$$

The  $t$ -contributions are suppressed in this limit (there is no tree-level diagram here). Observe how the association of each one-loop diagram with a certain tree diagram is different from the corresponding one in the large- $t$  limit.

Imposing the respective normalization conditions

$$B_s^{\phi\phi\phi\phi}(s = \kappa, t, \kappa) = B_u^{\phi\phi\phi\phi}(t, u = \kappa, \kappa) = \frac{g_B^2}{-\kappa} \quad (121)$$

and proceeding as before, we obtain the expected result

$$\tilde{\Gamma}_B^{\phi\phi\phi\phi}(s,t) = \frac{g_B^2}{-\kappa} \frac{1 + e^{i\pi\alpha(t)}}{Z(t, \kappa)} \left(\frac{s}{\kappa}\right)^{\alpha(t)}, \quad \alpha(t) = g_B^2 K_m(t) - 1 \quad (122)$$

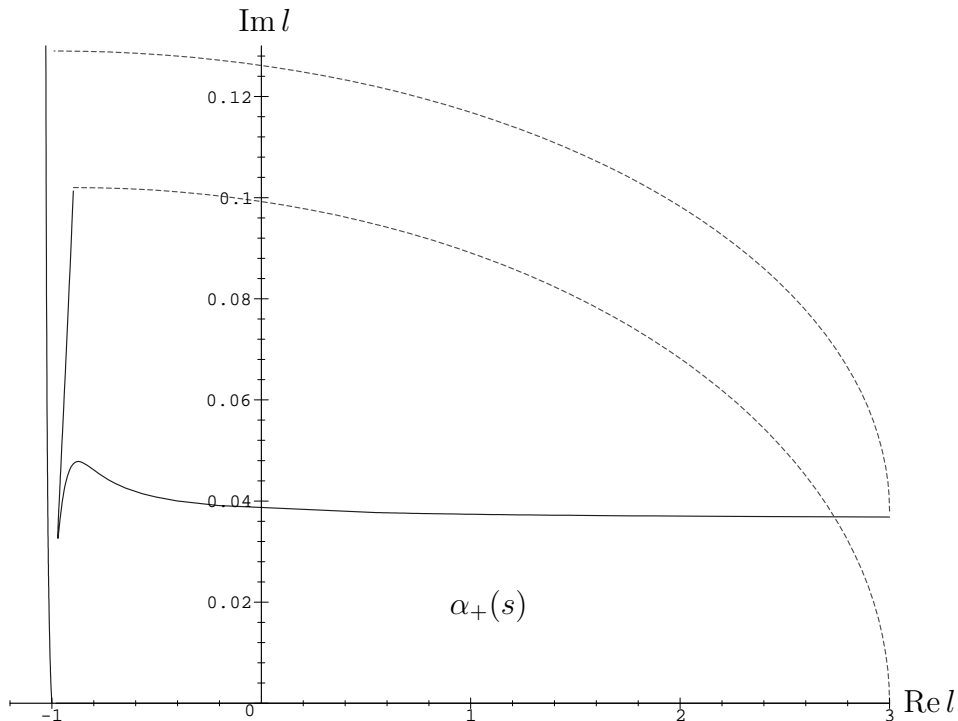


Figure 2: The trajectory  $\alpha_+$  for the zero charge sector in the complex  $l$ -plane for the values  $M = 1$ ,  $m = 2$  and  $g_B^2/(16\pi^2) = 1/25$ . The trajectory starts out at  $l = -1$  following the real axis to the right and goes off to infinity at  $s = 4M^2$  and  $s = 4m^2$  (represented by the dashed lines).

in the limit  $s \rightarrow \infty$ .

Let us conclude this section with a brief discussion of the Regge trajectories found in the present approximation. A much more exhaustive discussion of their qualitative and quantitative features will be given elsewhere. Of the trajectories found above,  $\alpha_+$  (in the sectors with charge one and zero) and  $\alpha_0 = \alpha$  correspond to attractive interactions, while the  $\alpha_-$ -trajectories are repulsive. The appearance of repulsive trajectories can be attributed to the presence of exchange interactions. The other salient qualitative feature is the divergence of the trajectories at  $s = 4M^2$ ,  $4m^2$  or  $(M + m)^2$  (depending on the charge sector), as can be read off from the explicit expression (84). This divergence at threshold is inappropriate in the case of interactions through exchange of massive particles and has to be considered a defect of the lowest order approximation. It would imply for instance the existence of an infinite number of bound states as realized in the case of zero mass exchange particles producing an interaction of infinite range (barring confinement, of course). Technically, the problem can be traced to the loss of information about the mass of the exchange particle in the process of taking the limit  $t \rightarrow \infty$ , as remarked below eq. (83). The mass of the exchange particle will enter at two loops, however, whether this is sufficient to cut off the spectrum at a finite number of bound states remains to be seen.

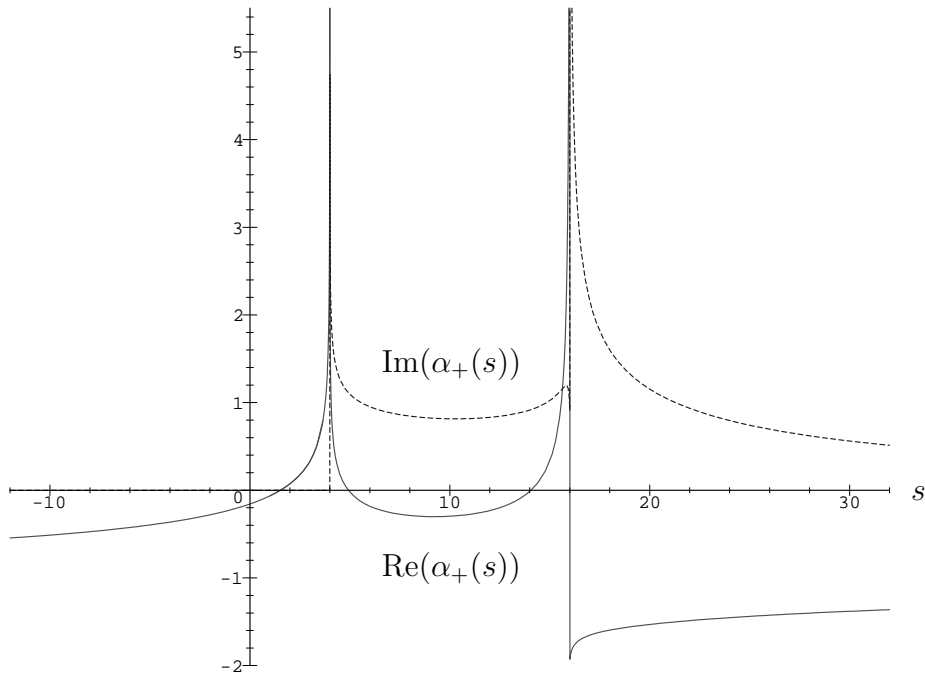


Figure 3: Real (solid line) and imaginary (dashed line) parts of  $\alpha_+$  as functions of  $s$  for the values  $M = 1$ ,  $m = 2$  and  $g_B^2/(16\pi^2) = 1$ . Note that the values of  $s$  where  $\text{Re}(\alpha_+(s))$  crosses an integer with negative slope do *not* correspond to physical states, but rather to so-called “ghost” states.

The trajectories  $\alpha_+$  in the charge one sector and  $\alpha_0 = \alpha$  show a qualitative behaviour similar to the “typical” trajectory depicted in fig. 1, except for the fact that they go off to infinity at threshold. Interestingly,  $\alpha_+$  in the zero charge sector behaves differently owing to the existence of two thresholds at  $4M^2$  and  $4m^2$ . Consequently, it produces two series of bound states and resonances (within ranges of values for the coupling constant) with overlapping angular momenta. The trajectory is represented in fig. 2 in the complex  $l$ -plane, while fig. 3 shows a plot of its real and imaginary parts as functions of  $s$ , so that the masses of bound states and resonances can in principle be read off from the points where  $\text{Re}(\alpha_+(s))$  equals an (even) positive integer. We have used different coupling constants in the two cases in order to make the overall qualitative features clearly visible.

The trajectory  $\alpha$  had been found before from the Bethe-Salpeter equation [21] and by direct summation of leading logs [22]. We can compare the bound state spectrum with a direct solution of the Bethe-Salpeter equation in the ladder approximation. For the Wick-Cutkosky model with a massless exchange particle we find good agreement for small values of the coupling constant. The other Regge trajectories  $\alpha_{\pm}$  represent new results and would have been very difficult to obtain from either the Bethe-Salpeter equation or a summation of leading logs (in the latter case due to the difficulty in determining the combinatorial factors of the diagrams in the charge zero sector to all orders).

## 6 Discussion and Conclusions

We have introduced and developed in this paper a methodology based on environmentally friendly renormalization for investigating high momentum behaviour in quantum field theory in the asymmetric case where  $t \gg s$  or  $s \gg t$ , i.e.  $x \ll 1$ . We have seen that renormalization in this limit introduces several rather novel features. First of all, we saw that it was necessary to introduce a renormalization to remove a finite term due to the fact that in the asymmetric limits  $t \rightarrow \infty$  for fixed  $s$ , or  $s \rightarrow \infty$  for fixed  $t$  the term is logarithmically divergent. We showed that to do this consistently and successfully in perturbation theory an overall renormalization of the Greens function or vertex function was not sufficient, rather one was obliged to identify appropriate subsets of diagrams contained in the Greens functions and renormalize them accordingly. An appropriate normalization condition then assured that as much as possible of the perturbative series was exponentiated via the RG. For a  $\phi^\dagger\phi\psi$  interaction we saw that due to mixing of the different four-point effective couplings it was necessary to implement a matrix renormalization.

The renormalizations we implemented naturally preserve crossing symmetry, an important advantage compared to the Bethe-Salpeter equation in the ladder approximation. In the case of a gauge theory our methodology would also naturally preserve gauge invariance, once again an advantage over the Bethe-Salpeter equation. We saw that an environmentally friendly RG could be used to derive a scaling form for the two-particle scattering amplitude that was formally the same as that derived by Regge theory. We then derived explicit scaling forms to one loop for a simple cubic theory and for a charged scalar field interacting with a neutral scalar field. In particular we derived the Regge trajectories for these theories to one loop, corresponding to the summation of all leading logs.

We were also able to extract the signatures of the Regge trajectories. Their physical significance from the viewpoint of the corresponding bound state and resonance physics, as well as related qualitative properties of the trajectories, will be discussed fully in a future publication. As far as quantitative implications are concerned, in the cases where a direct comparison can be made, our results are in good agreement with those of the Bethe-Salpeter equation when the mass of the exchange particle is small. For large masses there is a significant deviation, this disadvantage being associated with what is also the principle advantage of going to the Regge limit to examine bound state phenomena — the factorization of Feynman diagrams. It is this factorization that allowed for a simple multiplicative renormalization once the relevant functions that do multiplicatively renormalize were identified. Our results would thus seem to be more promising in this regard for theories with massless interchange such as QED, QCD and gravity.

Some extensions of the present work are immediate and will be treated in the very near future. Among them is the incorporation of particles with spin into the formalism, including the phenomenon of Reggeization for spin one-half fermions. The methodology presented in this paper appears to be equally applicable to theories with fermions and/or gauge bosons, the key being to identify the subsets of diagrams that need renormalization due to their divergent behaviour in the high-momentum limit. Another point is the formal divergence of the trajectories for massless particles propagating in the non-contracted direction. Here an implicit equation for the Regge trajectory like the one found by Polkinghorne [23] through

summation of all logs of ladder diagrams could turn out to be important. Of course, within our framework it should be established from RG arguments. Such an equation, and the extension to higher loop orders, may also be important in resolving the issue of the independence of the trajectories to one-loop order with respect to the mass of the exchange particle.

Let us finally comment on some other interesting aspects of the present formalism, which we plan to explore in future applications. One noteworthy property is the “duality” implicit in our renormalization. We saw that it was possible to use the RG to resum the “dual” limits  $s \rightarrow \infty, t$  fixed and  $t \rightarrow \infty, s$  fixed yielding in these asymptotic limits behaviour of the form  $s^{\alpha(t)}$  and  $t^{\alpha(s)}$  respectively. In these limits the RG sums up “dual” sets of ladder diagrams, however, each limit requires a different normalization condition. Naturally, it would be very interesting to look for a uniform renormalization that accesses both dual limits at one and the same time.

Another interesting aspect of our methodology is the ability to access the kinematic dimensional reduction characteristic of the Regge limit. This limit is not only of interest in a theory such as QCD but also could have a very important role to play in quantum gravity as has been emphasized by 't Hooft [24], and especially in the question of black hole formation as has been advocated in ref. [25] where the use of an RG that is capable of coarse graining between “hard” particles (that contribute to the background metric of the black hole) and “soft” particles (that represent particle production on the background metric) has been proposed as a method for understanding the physics of gravitational collapse and proving that it is governed by a unitary evolution. We hope that the type of RG exhibited in this paper may prove to be a first step in this direction.

In work related to the above, 't Hooft [26] also showed that certain Planck scale processes can be calculated using known laws of physics. Specifically scattering processes with  $s \gg t$  can be calculated which lead to scattering amplitudes that have certain features in common with string theory scattering amplitudes. This work was extended by the Verlindes [27] who showed that in the “Regge” regime quantum gravity separates into strongly coupled (longitudinal) and weakly coupled (transverse) sectors. The methodology used was basically an eikonal type approximation. For a scalar theory such as we have considered here the eikonal approximation is trivial in the limit  $s \rightarrow \infty$  for fixed  $t$ ; the contributions of ladder diagrams that are two-particle irreducible in the  $t$ -channel yield a Born type limit, whilst ladder diagrams that are two-particle irreducible in the  $s$ -channel lead to non-trivial Regge behaviour. This is obviously a matter that depends very much on the spin of the interchange particle and is one we will return to in the future.

## Acknowledgements

It is a pleasure to thank U. Ellwanger and D. O'Connor for interesting and helpful discussions. We would also like to thank S. Dilcher for help with the graphics and reading of the manuscript.



## Appendix A

In this appendix we will formally give the two-loop results, showing that the renormalization schemes proposed are consistent to two-loop level. We will consider explicitly only the simplest case of a  $\phi^3$  theory. For  $B_{B,t}$  we have in the large- $t$  limit to two loops

$$\begin{aligned}
 B_{B,t}(s, t) &= \frac{g_B^2}{-t} + \frac{g_B^4}{-t} K(s) \ln(-t) + \frac{g_B^6}{-2t} K^2(s) \ln^2(-t) \\
 &\quad + \frac{g_B^6}{-t} K'(s) \ln(-t) + O\left(\frac{g_B^4}{t}, \frac{g_B^6}{t}\right)
 \end{aligned} \tag{123}$$

with  $-t = e^{i\pi}t$  and  $K(s)$  and  $K'(s)$  as in section 3. Using the normalization condition (48),

$$B_t(s, t = \kappa, \kappa) = \frac{g_B^2}{-\kappa},$$

one finds

$$Z_t(s, \kappa) = 1 - g_B^2 K(s) \ln(-\kappa) + \frac{g_B^4}{2} K^2(s) \ln^2(-\kappa) - g_B^4 K'(s) \ln(-\kappa). \tag{124}$$

Hence, the renormalized function  $B_t$  (before applying the RG) is given by

$$B_t(s, t, \kappa) = \frac{g_B^2}{-t} + \frac{g_B^4}{-t} K(s) \ln\left(\frac{t}{\kappa}\right) + \frac{g_B^6}{-2t} K^2(s) \ln^2\left(\frac{t}{\kappa}\right) + \frac{g_B^6}{-t} K'(s) \ln\left(\frac{t}{\kappa}\right). \tag{125}$$

As long as the arbitrary scale,  $\kappa$ , is chosen such that  $g_B^2 \ln(t/\kappa) \ll 1$  then perturbative expressions will be well defined, i.e. that our proposed renormalization also works to two-loop order. Utilizing the RG, to two loops one finds

$$\gamma_t(s) = -g_B^2 K(s) - g_B^4 K'(s), \tag{126}$$

so the result for the  $t$ -contributions is

$$B_t(s, t, \kappa) = \frac{g_B^2}{-\kappa} \left(\frac{t}{\kappa}\right)^{\alpha(s)}, \quad \alpha(s) = g_B^2 K(s) + g_B^4 K'(s) - 1. \tag{127}$$

The analogous two-loop calculation for  $B_u$  goes through in exactly the same way, showing that the trajectory has positive signature as expected.

## Appendix B

In this part we demonstrate that the one-loop renormalization scheme presented in sections 3 and 4 sums the leading logs to all orders in perturbation theory. We consider the large- $t$  limit and give the proof explicitly for the charge zero sector in  $\phi^\dagger\phi\psi$  theory. It will be apparent that the same arguments hold in all other cases, too.

It can be shown in general for scalar theories that at a given loop order the diagrams giving the highest power of  $\ln t$  are the ladder diagrams in  $s$ -direction. More specifically,

a ladder with  $k$  loops leads to a contribution of the form  $\sim (g_B^{2k+2}/k!) t^{-1} K^k(s) (\ln t)^k$  (see e.g. ref. [4]). For the  $t$ -contributions, the ladders in question are planar diagrams with  $k+1$  “d-lines”, whose contraction leaves a product of factorized two-dimensional bubbles  $K(s)$ . Depending on the specific theory, not necessarily all the  $K$ ’s represent the same function.

In general it is difficult to write down a formula for the leading contributions to all orders, including all contributing planar ladder diagrams and their combinatorial factors, and in particular this is the case for the  $\phi^\dagger\phi\psi$  theory under consideration. Nevertheless, it is relatively easy to give a recursive prescription, generating the contribution to  $k+1$  loops from the  $k$ -loop term just by adding one further rung to the ladder in every possible way. In this way we will show that the solution (65) of the RG equation,

$$\mathbf{B}_t(s, t, \kappa) = \frac{g_B^2}{-t} \sum_{k=0}^{\infty} \frac{g_B^{2k}}{k!} \ln^k(-t) (\mathbf{b}_1(s) \mathbf{b}_0^{-1})^k \mathbf{b}_0, \quad (128)$$

produces the correct contributions to every loop order. We have replaced  $\ln(t/\kappa)$  by  $\ln(-t)$  here since the  $\kappa$ -dependence does not arise in perturbation theory without renormalization, and in any case  $\ln(-\kappa)$  is negligible compared to  $\ln(-t)$  in the large- $t$  limit. In particular  $\mathbf{Z}_t$  does not contribute to the leading logs in  $t$ , so that  $\mathbf{B}_t = \mathbf{B}_{B,t}$  in the leading log approximation.

From (128) we deduce that our renormalization scheme yields the recursive formula

$$\mathbf{B}_t^{(k+1)}(s, t, \kappa) = \frac{g_B^2}{k+1} \ln(-t) \mathbf{b}_1(s) \mathbf{b}_0^{-1} \mathbf{B}_t^{(k)}(s, t, \kappa), \quad (129)$$

where  $\mathbf{B}_t^{(k)}$  stands for the  $k$ -loop term. Referring to the definition (60) of  $\mathbf{b}_0$  and  $\mathbf{b}_1$ , we see that the tree-level term is correctly reproduced by (128), and we have to look at the action of the matrix

$$g_B^2 \ln(-t) \mathbf{b}_1(s) \mathbf{b}_0^{-1} = -\ln(-t) \boldsymbol{\gamma}_t(s) = g_B^2 \ln(-t) \begin{pmatrix} K_m(s) & 0 & K_M(s) \\ 0 & K_m(s) & K_M(s) \\ K_m(s) & K_m(s) & 0 \end{pmatrix} \quad (130)$$

in (129) (cf. (106) for the explicit form of  $\boldsymbol{\gamma}_t$ ).

We may represent this matrix graphically as follows:

$$g_B^2 \ln(-t) \mathbf{b}_1(s) \mathbf{b}_0^{-1} = \begin{pmatrix} \begin{array}{ccc} \text{Diagram 1} & 0 & \text{Diagram 2} \\ 0 & \text{Diagram 3} & \text{Diagram 4} \\ \text{Diagram 5} & \text{Diagram 6} & 0 \end{array} \end{pmatrix}, \quad (131)$$

indicating that its action consists in closing the outgoing legs of the  $k$ -loop terms into two-dimensional loops and adding the correct upper legs for the  $(k+1)$ -loop terms. Note that the

lower vertices indicated in the diagrams are already present in the  $k$ -th terms, while the upper vertices are added to yield the next terms. As an illustration, consider the action of (131) on the tree-level terms producing the  $\phi^\dagger\phi\phi^\dagger\phi$ -entry of the matrix of one-loop contributions,

$$\text{Diagram 1} \times \text{Diagram 2} + \text{Diagram 3} \times \text{Diagram 4} = \text{Diagram 5} + \text{Diagram 6} \quad (132)$$

(see the next appendix for a diagrammatic representation of  $\mathbf{b}_0$  and  $\mathbf{b}_1$ ).

It is obvious that (131) produces all possible terms at  $(k+1)$ -loop order from the  $k$ -loop terms, thus establishing the correctness of the leading logs in (128) to all orders by induction. To see that the same argument holds for every scalar theory, observe that the matrix corresponding to (131) in the theory considered is uniquely fixed by the way it produces the one-loop from the tree contributions (provided that  $\mathbf{b}_0$  is invertible, what we assume here). It will then yield the  $(k+1)$ -th term from the  $k$ -th term for every  $k$ .

Turning finally to the  $u$ -contributions, we have to establish that the counterpart to (128),

$$\mathbf{B}_u(s, t, \kappa) = \frac{g_B^2}{t} \sum_{k=0}^{\infty} \frac{g_B^{2k}}{k!} (\ln t)^k (\mathbf{b}'_1(s) \mathbf{b}'_0{}^{-1})^k \mathbf{b}'_0, \quad (133)$$

reproduces correctly the leading logs in  $t$  for the  $u$ -contributions. The argument is identical to the above for the  $t$ -contributions, taking into account eq. (72),

$$\mathbf{b}'_1(s) \mathbf{b}'_0{}^{-1} = \mathbf{b}_1(s) \mathbf{b}_0{}^{-1}.$$

The only difference between  $\mathbf{B}_u$  and  $\mathbf{B}_t$  is then (besides the substitution  $-t \rightarrow t$ ) in the change of the tree-level matrix  $\mathbf{b}_0 \rightarrow \mathbf{b}'_0$ . This is entirely reasonable since on a diagrammatic level it amounts to crossing the incoming legs for the full series  $\mathbf{B}_t$ . This remark concludes the proof.

## Appendix C

In this appendix we will collect together some miscellaneous formulas needed in the calculation of the charge zero sector in section 5. First of all we give the diagrams for the  $t$ -contributions in one-loop perturbation theory:

$$\mathbf{B}_{B,t}(s, t) = \begin{pmatrix} \text{Diagram 1} & 0 & \text{Diagram 2} \\ 0 & \text{Diagram 3} & \text{Diagram 4} \\ \text{Diagram 5} & \text{Diagram 6} & 0 \end{pmatrix}$$

$$+ \left( \begin{array}{ccc} \begin{array}{c} \text{Diagram 1} + \text{Diagram 2} \\ \text{Diagram 3} \\ \text{Diagram 4} \end{array} & \begin{array}{c} \text{Diagram 5} + \text{Diagram 6} \\ \text{Diagram 7} \end{array} & \begin{array}{c} \text{Diagram 8} \\ \text{Diagram 9} + \text{Diagram 10} \end{array} \end{array} \right) \quad (134)$$

In the limit  $t \rightarrow \infty$ , these diagrams get contracted to yield

$$\mathbf{B}_{B,t}(s, t) = \left( \begin{array}{ccc} \begin{array}{c} \text{Diagram 1} \\ \text{Diagram 2} \end{array} & 0 & \begin{array}{c} \text{Diagram 3} \\ \text{Diagram 4} \end{array} \\ 0 & \begin{array}{c} \text{Diagram 5} \\ \text{Diagram 6} \end{array} & \begin{array}{c} \text{Diagram 7} \\ \text{Diagram 8} \end{array} \\ \begin{array}{c} \text{Diagram 9} \\ \text{Diagram 10} \end{array} & \begin{array}{c} \text{Diagram 11} \\ \text{Diagram 12} \end{array} & 0 \end{array} \right)$$

$$+ \left( \begin{array}{ccc} \begin{array}{c} \text{Diagram 13} + \text{Diagram 14} \\ \text{Diagram 15} \\ \text{Diagram 16} \end{array} & \begin{array}{c} \text{Diagram 17} + \text{Diagram 18} \\ \text{Diagram 19} \end{array} & \begin{array}{c} \text{Diagram 20} \\ \text{Diagram 21} + \text{Diagram 22} \end{array} \end{array} \right) \quad (135)$$

leading to the analytic expressions in (105).

The normalization condition

$$\mathbf{B}_t(s, t = \kappa, \kappa) = \frac{g_B^2}{-\kappa} \begin{pmatrix} 1 & 0 & 1 \\ 0 & 1 & 1 \\ 1 & 1 & 0 \end{pmatrix} \quad (136)$$

gives

$$\mathbf{Z}_t(s, \kappa) = \begin{pmatrix} 1 & 0 & 0 \\ 0 & 1 & 0 \\ 0 & 0 & 1 \end{pmatrix} - g_B^2 \ln(e^{-i\pi} \kappa) \begin{pmatrix} K_m(s) & 0 & K_M(s) \\ 0 & K_m(s) & K_M(s) \\ K_m(s) & K_m(s) & 0 \end{pmatrix}, \quad (137)$$

hence we arrive at the  $\gamma_t$  in (106),

$$\gamma_t(s) = -g_B^2 \begin{pmatrix} K_m(s) & 0 & K_M(s) \\ 0 & K_m(s) & K_M(s) \\ K_m(s) & K_m(s) & 0 \end{pmatrix}.$$

Its (unnormalized) eigenvectors and corresponding eigenvalues are

$$\begin{aligned}
\mathbf{v}_+(s) &= \begin{pmatrix} 1 + \left(1 + 8 \frac{K_M(s)}{K_m(s)}\right)^{\frac{1}{2}} \\ 1 + \left(1 + 8 \frac{K_M(s)}{K_m(s)}\right)^{\frac{1}{2}} \\ 4 \end{pmatrix}, & \gamma_+(s) &= -\frac{g_B^2 K_m(s)}{2} \left(1 + \left(1 + 8 \frac{K_M(s)}{K_m(s)}\right)^{\frac{1}{2}}\right), \\
\mathbf{v}_-(s) &= \begin{pmatrix} 1 - \left(1 + 8 \frac{K_M(s)}{K_m(s)}\right)^{\frac{1}{2}} \\ 1 - \left(1 + 8 \frac{K_M(s)}{K_m(s)}\right)^{\frac{1}{2}} \\ 4 \end{pmatrix}, & \gamma_-(s) &= -\frac{g_B^2 K_m(s)}{2} \left(1 - \left(1 + 8 \frac{K_M(s)}{K_m(s)}\right)^{\frac{1}{2}}\right), \\
\mathbf{v}_0(s) &= \begin{pmatrix} -1 \\ 1 \\ 0 \end{pmatrix}, & \gamma_0(s) &= -g_B^2 K_m(s).
\end{aligned} \tag{138}$$

The solution of the RG equation yields for  $\mathbf{B}_t$

$$\begin{aligned}
B_t^{\phi^\dagger \phi \phi^\dagger \phi}(s, t, \kappa) &= B_t^{\phi \phi^\dagger \phi \phi^\dagger}(s, t, \kappa) \\
&= -\frac{g_B^2}{\kappa} C_+(s) \left(\frac{t}{\kappa}\right)^{\alpha_+(s)} - \frac{g_B^2}{\kappa} C_-(s) \left(\frac{t}{\kappa}\right)^{\alpha_-(s)} - \frac{g_B^2}{2\kappa} \left(\frac{t}{\kappa}\right)^{\alpha_0(s)}, \\
B_t^{\phi^\dagger \phi \phi \phi^\dagger}(s, t, \kappa) &= B_t^{\phi \phi^\dagger \phi^\dagger \phi}(s, t, \kappa) \\
&= -\frac{g_B^2}{\kappa} C_+(s) \left(\frac{t}{\kappa}\right)^{\alpha_+(s)} - \frac{g_B^2}{\kappa} C_-(s) \left(\frac{t}{\kappa}\right)^{\alpha_-(s)} + \frac{g_B^2}{2\kappa} \left(\frac{t}{\kappa}\right)^{\alpha_0(s)}, \\
B_t^{\phi^\dagger \phi \psi \psi}(s, t, \kappa) &= B_t^{\phi \phi^\dagger \psi \psi}(s, t, \kappa) = B_t^{\psi \psi \phi^\dagger \phi}(s, t, \kappa) = B_t^{\psi \psi \phi \phi^\dagger}(s, t, \kappa) \\
&= -\frac{g_B^2}{\kappa} D_+(s) \left(\frac{t}{\kappa}\right)^{\alpha_+(s)} - \frac{g_B^2}{\kappa} D_-(s) \left(\frac{t}{\kappa}\right)^{\alpha_-(s)}, \\
B_t^{\psi \psi \psi \psi}(s, t, \kappa) &= -\frac{g_B^2}{\kappa} E(s) \left(\frac{t}{\kappa}\right)^{\alpha_+(s)} + \frac{g_B^2}{\kappa} E(s) \left(\frac{t}{\kappa}\right)^{\alpha_-(s)},
\end{aligned} \tag{139}$$

with the amplitude functions

$$C_\pm(s) = \frac{1}{4} \left( 1 \pm \frac{1 + 4 \frac{K_M(s)}{K_m(s)}}{\sqrt{1 + 8 \frac{K_M(s)}{K_m(s)}}} \right),$$

$$\begin{aligned}
D_{\pm}(s) &= \frac{1}{2} \left( 1 \pm \frac{1}{\sqrt{1 + 8 \frac{K_M(s)}{K_m(s)}}} \right), \\
E(s) &= \frac{2}{\sqrt{1 + 8 \frac{K_M(s)}{K_m(s)}}},
\end{aligned} \tag{140}$$

and the Regge trajectories from (114),

$$\begin{aligned}
\alpha_{\pm}(s) &= \frac{g_B^2 K_m(s)}{2} \left( 1 \pm \left( 1 + 8 \frac{K_M(s)}{K_m(s)} \right)^{\frac{1}{2}} \right) - 1, \\
\alpha_0(s) &= g_B^2 K_m(s) - 1.
\end{aligned}$$

Now for the  $u$ -contributions the diagrams up to one loop are

$$\begin{aligned}
\mathbf{B}_{B,u}(s, t) &= \left( \begin{array}{ccc} 0 & \text{diagram} & \text{diagram} \\ \text{diagram} & 0 & \text{diagram} \\ \text{diagram} & \text{diagram} & 0 \end{array} \right) \\
&+ \left( \begin{array}{ccc} \text{diagram} & \text{diagram} + \text{diagram} & \text{diagram} \\ \text{diagram} + \text{diagram} & \text{diagram} & \text{diagram} \\ \text{diagram} & \text{diagram} & \text{diagram} + \text{diagram} \end{array} \right) \tag{141}
\end{aligned}$$

The contracted diagrams in the limit  $u \rightarrow \infty$  lead to the same analytic expressions as in (105) for the  $t$ -contributions, except that the first and second column (or row) are interchanged (and  $t$  is replaced by  $u$ ). With the normalization condition

$$\mathbf{B}_u(s, u = \kappa, \kappa) = \frac{g_B^2}{-\kappa} \begin{pmatrix} 0 & 1 & 1 \\ 1 & 0 & 1 \\ 1 & 1 & 0 \end{pmatrix} \tag{142}$$

we then find  $\mathbf{Z}_u = \mathbf{Z}_t$  and  $\gamma_u = \gamma_t$ . The results for  $\mathbf{B}_u$  read

$$\begin{aligned}
B_u^{\phi^\dagger \phi \phi^\dagger \phi}(s, u, \kappa) &= B_u^{\phi \phi^\dagger \phi \phi^\dagger}(s, u, \kappa) \\
&= -\frac{g_B^2}{\kappa} C_+(s) \left( \frac{u}{\kappa} \right)^{\alpha_+(s)} - \frac{g_B^2}{\kappa} C_-(s) \left( \frac{u}{\kappa} \right)^{\alpha_-(s)} + \frac{g_B^2}{2\kappa} \left( \frac{u}{\kappa} \right)^{\alpha_0(s)},
\end{aligned}$$

$$\begin{aligned}
B_u^{\phi^\dagger\phi\phi^\dagger}(s, u, \kappa) &= B_u^{\phi^\dagger\phi^\dagger\phi}(s, u, \kappa) \\
&= -\frac{g_B^2}{\kappa} C_+(s) \left(\frac{u}{\kappa}\right)^{\alpha_+(s)} - \frac{g_B^2}{\kappa} C_-(s) \left(\frac{u}{\kappa}\right)^{\alpha_-(s)} - \frac{g_B^2}{2\kappa} \left(\frac{u}{\kappa}\right)^{\alpha_0(s)}, \\
B_u^{\phi^\dagger\phi\psi\psi}(s, u, \kappa) &= B_u^{\phi^\dagger\psi\psi}(s, u, \kappa) = B_u^{\psi\psi\phi^\dagger}(s, u, \kappa) = B_u^{\psi\psi\phi^\dagger}(s, u, \kappa) \\
&= -\frac{g_B^2}{\kappa} D_+(s) \left(\frac{u}{\kappa}\right)^{\alpha_+(s)} - \frac{g_B^2}{\kappa} D_-(s) \left(\frac{u}{\kappa}\right)^{\alpha_-(s)}, \\
B_u^{\psi\psi\psi\psi}(s, u, \kappa) &= -\frac{g_B^2}{\kappa} E(s) \left(\frac{u}{\kappa}\right)^{\alpha_+(s)} + \frac{g_B^2}{\kappa} E(s) \left(\frac{u}{\kappa}\right)^{\alpha_-(s)}. \tag{143}
\end{aligned}$$

Finally, the (finite)  $s$ -contributions are

$$\mathbf{B}_s(s) = \begin{pmatrix} \begin{array}{c} \text{Diagram 1} \\ \text{Diagram 2} \\ \text{Diagram 3} \\ \text{Diagram 4} \\ 0 \end{array} & \begin{array}{c} \text{Diagram 5} \\ \text{Diagram 6} \\ \text{Diagram 7} \\ \text{Diagram 8} \\ 0 \end{array} & \begin{array}{c} 0 \\ 0 \\ 0 \\ 0 \end{array} \end{pmatrix} = \frac{g_B^2}{M^2 - s} \begin{pmatrix} 1 & 1 & 0 \\ 1 & 1 & 0 \\ 0 & 0 & 0 \end{pmatrix}. \tag{144}$$

Adding all the contributions leads to the scattering amplitudes of eqs. (110–113).

## References

- [1] G. Altarelli, *Phys. Rep.* **81** (1982) 1.
- [2] M. Derrick et al., *Z. Phys.* **C69** (1996) 607.
- [3] E.A. Kuraev, L.N. Lipatov and V.S. Fadin, *Sov. Phys. JETP* **45** (1977) 199.
- [4] R.J. Eden, P.V. Landshoff, D.I. Olive and J.C. Polkinghorne, “*The Analytic S-Matrix*”, Cambridge University Press 1966.
- [5] L. Bertocchi, S. Fubini and M. Tonin, *Nuovo Cim.* **25** (1962) 626;  
D. Amati, A. Stanghellini and S. Fubini, *Nuovo Cim.* **26** (1962) 6.
- [6] A. Schwimmer, *Nucl. Phys.* **B75** (1974) 446.
- [7] M. Levy and J. Sucher, *Phys. Rev.* **186** (1969) 1656.
- [8] C.R. Stephens, A. Weber, J.C. López Vieyra and P.O. Hess, *Phys. Lett.* **B414** (1997) 333.
- [9] A.A. Migdal, A.M. Polyakov and K.A. Ter-Martirosyan, *Phys. Lett.* **B48** (1974) 239.
- [10] C.R. Stephens, *Mod. Phys. Lett.* **A12** (1997) 2905.

- [11] D. O'Connor and C.R. Stephens, *Nucl. Phys.* **B360** (1991) 297; *Int. J. Mod. Phys.* **A9** (1994) 2805; *Phys. Rev. Lett.* **72** (1994) 506.
- [12] D. O'Connor, C.R. Stephens and F. Freire, *Mod. Phys. Lett.* **A8** (1993) 1779; M.A. van Eijck, C.R. Stephens and C.G. van Weert, *Mod. Phys. Lett.* **A9** (1994) 309.
- [13] Yu.V. Novozhilov, “*Introduction to Elementary Particle Theory*”, Pergamon Press, Oxford 1975; R.J. Eden, “*High Energy Collisions of Elementary Particles*”, Cambridge University Press 1967.
- [14] M. Froissart, talk at La Jolla Conference 1961 (unpublished); V.N. Gribov, *Sov. Phys. JETP* **15** (1962) 873; S.C. Frautschi, M. Gell-Mann and F. Zachariasen, *Phys. Rev.* **126** (1962) 2204; J. Challifour and R.J. Eden, *Phys. Rev.* **129** (1963) 2349.
- [15] E.C. Titchmarsh, “*The Theory of Functions*”, 2nd edition, Oxford University Press 1939; R.P. Boas, “*Entire Functions*”, Academic Press, New York 1954.
- [16] G.N. Watson, *Proc. Roy. Soc.* **95** (1918) 83; A. Sommerfeld, “*Partial Differential Equations in Physics*”, Academic Press, New York 1949.
- [17] T. Regge, *Nuovo Cim.* **14** (1959) 951; *ibid.* **18** (1960) 947.
- [18] Bateman Manuscript Project, “*Higher Transcendental Functions*”, Vol. I, ed. A. Erdelyi, McGraw-Hill, New York 1953.
- [19] C.R. Stephens, “*Why Two Renormalization Groups are Better than One*”, UNAM preprint ICN-UNAM-96-11, hep/th-9611062; C. Ford and C. Weisendanger, *Phys. Lett.* **B398** (1997) 342; *Phys. Rev.* **D55** (1997) 2202.
- [20] H.D.I. Abarbanel, *Rev. Mod. Phys.* **48** (1976) 435.
- [21] B.W. Lee and R.F. Sawyer, *Phys. Rev.* **127** (1962) 2266.
- [22] J.C. Polkinghorne, *J. Math. Phys.* **4** (1963) 503; P.G. Federbush and M.T. Grisaru, *Ann. Phys.* **22** (1963) 263, 299.
- [23] J.C. Polkinghorne, *J. Math. Phys.* **5** (1964) 431.
- [24] G. 't Hooft, in “*Salamfestschrift*”, eds. A. Ali, J. Ellis and S. Randjbar-Daemi, World Scientific 1993.
- [25] C.R. Stephens, G. 't Hooft and B. Whiting, *Class. Quan. Grav.* **11** (1994) 621.
- [26] G. 't Hooft, *Phys. Lett.* **B198** (1987) 61.
- [27] E. Verlinde and H. Verlinde, *Nucl. Phys.* **B371** (1992) 246.